J. Fluid Mech. (2014), *vol.* 738, *pp.* 65–104. © Cambridge University Press 2013
doi:10.1017/jfm.2013.584

Trapped waves on jet currents: asymptotic modal approach

Victor I. Shrira[1,†] **and Alexey V. Slunyaev**[1,2,3]

[1]Department of Mathematics, EPSAM, Keele University, Keele ST5 5BG, UK

[2]Department of Nonlinear Geophysical Processes, Institute of Applied Physics, 46 Ulyanova Street, N. Novgorod 603950, Russia

[3]Nizhny Novgorod State Technical University, 24 Minina Street, N. Novgorod 603950, Russia

(Received 15 October 2012; revised 14 September 2013; accepted 30 October 2013; first published online 2 December 2013)

An asymptotic theory of surface waves trapped on vertically uniform jet currents is developed as a first step towards a systematic description of wave dynamics on oceanic jet currents. It has been shown that in a linear setting an asymptotic separation of vertical and horizontal variables, which underpins the modal description of the wave field on currents, is possible if either the current velocity is small compared to the wave celerity or the current width is large compared to the wavelength along the current. The scheme developed enables us to obtain solutions as an asymptotic series with any desired accuracy. The initially three-dimensional problem is reduced to solving one-dimensional equations with the lateral and vertical dependence being prescribed by the corresponding modal structure. To leading order in current magnitude to wave celerity, the boundary value problem specifying the modes and eigenvalues reduces to classical Sturm–Liouville type based upon the one-dimensional stationary Schrödinger equation. The modes, both trapped and 'passing-through', form a complete orthogonal set. This makes the modal description of waves on currents a mathematically attractive alternative to the approaches currently adopted. Properties of trapped eigenmodes and their dispersion relations are examined both for broad currents of arbitrary magnitude, where the modes are not orthogonal, and for weak currents, where the modes are orthogonal. Several model profiles for which nice analytical solutions of the leading-order boundary value problem are known were used to get an insight. The asymptotic solutions proved not only to capture qualitative behaviour well but also to provide a good quantitative description even for unrealistically strong and narrow currents. The results are discussed for various oceanic currents, with particular attention paid to the Agulhas Current, for which specific estimates were derived. For typical dominant wind waves and swell, all oceanic-jet-type currents are weak and, correspondingly, the developed asymptotic scheme based upon one-dimensional stationary Schrödinger equation for modes applies.

Key words: surface gravity waves, waves/free-surface flows, wind–wave interactions

† Email address for correspondence: v.i.shrira@keele.ac.uk

https://doi.org/10.1017/jfm.2013.584 Published online by Cambridge University Press

1. Introduction

The original motivation for undertaking this study was to understand mechanisms resulting in a higher probability of anomalous or freak waves on currents, a fact known from the 1970s (Mallory 1974). To this end we re-examine the fundamentals of the wave–current interaction problem for waves on jet-like currents. Complementing the vast body of theoretical work devoted to waves on currents (see e.g. the reviews and books by Peregrine 1976; Thomas 1981; Jonsson 1990; Thomas & Klopman 1997; Lavrenov 2003; Bühler 2009) we focus our consideration upon waves trapped by jet currents. We will be primarily interested in the dominant wind waves and swell in the ocean.

The wide separation of scales between waves and currents has been the key assumption underlying the overwhelming majority of theoretical studies of wave fields on jet currents. Various versions of the WKB description enabled a picture of wave field evolution in a linear setting to be established by the mid-1970s (see e.g. reviews Peregrine 1976; Jonsson 1990). In this framework it is natural to distinguish three types of waves on jet currents: (i) 'passing-through' waves, which exist on the whole plane and refract while passing through the jet; (ii) 'reflected' waves, which are incident from infinity and then reflected by the jet; (iii) 'trapped' waves, which propagate inside the jet experiencing multiple reflections. A detailed discussion of the ray tracing picture, with a special emphasis on trapped waves, can be found in Kenyon (1971), for example. In the vicinity of isolated turning points, where the standard WKB description is invalid, it has to be complemented by a matched asymptotics approach, which yields a uniformly valid solution for the wave field (e.g. McKee 1974; Smith 1975; Peregrine 1976). Within the framework of such an approach, a wave field is described by a superposition of wave packets that are monochromatic in frequency, with local wave vectors varying because of wave refraction; the evolution of wave amplitude is being prescribed by the conservation of wave action. The approach was extended to narrow-banded weakly nonlinear fields. Under some additional assumptions, in particular, ensuring that the variations of the carrier wavenumber are sufficiently small, various versions of the nonlinear Schrödinger equation (NLS) were derived and analysed (Smith 1976; Turpin, Benmoussa & Mei 1983; Gerber 1987; Stocker & Peregrine 1999; Hjelmervik & Trulsen 2009; Onorato, Proment & Toffoli 2011; Ruban 2012). Note that Smith (1976) examined the wave field near caustics caused by reflection by an inhomogeneous current; in all later works there was no reflection.

The limitations of the above approaches did not receive due attention in the literature. First, note that even in the linear setting the WKB approach can only describe trapped waves qualitatively, since for low mode numbers the two turning points are too close to be treated as isolated turning points. In other words, the smallness of the characteristic wavelength compared to the scale of the current does not guarantee validity of the WKB approach, especially for waves propagating at small angles to the current. The situation is much worse when wave field nonlinear dynamics is considered: there is a fundamental obstacle which prevents the development of a consistent description of wave nonlinear dynamics on currents, even if wave refraction due to current inhomogeneity is well captured in the WKB approach in the linear limit. The wave nonlinear dynamics of typical broad-band wave fields occurs due to nonlinear resonant interactions, so it is natural to consider such interactions in the wavevector rather than in $\boldsymbol{x}$-space. There is no technique enabling description of wave resonant interactions in $\boldsymbol{x}$-space. The commonly adopted way of describing the nonlinear evolution of random broad-band fields on currents is based on the

https://doi.org/10.1017/jfm.2013.584 Published online by Cambridge University Press

Hasselmann equation, modified by a slowly varying current in such a way that the nonlinear term, i.e. the collision integral, remains the same as if there were no current and the wave motions were strictly potential (e.g. Komen *et al.* 1996; Lavrenov 2003). It can be argued that such an approach, although theoretically inconsistent, could be used to describe wave field evolution in the limit when the characteristic spatial scale of nonlinear interactions, L_{Nl}, which is $\sim\varepsilon^{-4}$ wavelengths, is much smaller than the scale of the current inhomogeneity L. It is easy to see that $L_{Nl} \sim 10^3$ km for typical wind waves: even if we take as the characteristic spatial scale of nonlinear interactions the scale of coherent interaction, $L_{Nl\ coherent}$, which is $\sim\varepsilon^{-2}$ wavelengths, it would give $L_{Nl\ coherent} \sim 10^1$ and 10^2 km for wind waves and swell, respectively. *A priori* it is not clear if there is room for the regime requiring $L_{Nl}, L_{Nl\ coherent} \ll L$ for the commonly used approach to be justified. The boundaries of such a regime have not been delineated, and it is not known how to describe wave field nonlinear evolution when the condition is violated. To our knowledge the very existence of this major gap in understanding has not been reflected in the literature.

We aim to address this gap and develop a systematic theoretical approach to weakly nonlinear waves on jet currents. In our context the term 'jet currents' is used for nearly parallel laterally localized currents with the characteristic cross-current scale much smaller than the scale of the longitudinal variation. There is a huge variety of such currents in nature, differing in scales and origin; we aim to develop a theoretical framework valid for arbitrary wave fields and the maximally wide range of geophysically relevant situations.

The main underlying idea we put forward is as follows. If the jet currents are longitudinally uniform, which is a reasonable first approximation, then solutions to the linearized equations of hydrodynamics for free water waves could always be presented in a separable form: as waves propagating along the current with some 'modal' dependence on the vertical and transverse variables. A modal description of linear waves on currents not relying on the WKB method was pioneered in the 1970s by Smith (1970) and Peregrine & Smith (1975) as a way to tackle specific problems. Even in the linear setting the modal description does have some advantages compared to the more commonly used WKB description: there are always trapped modes not tractable with the WKB method, and scale separation between the waves and current might not be large enough for the WKB method to be valid; however, the choice of approach is often a matter of convenience. For weakly nonlinear waves the situation is radically different: the modal description enables one to develop a systematic weakly nonlinear theory of wave interactions on jet currents, while the alternatives are applicable only under strong additional assumptions on the scale separation between the wave interaction scales and currents. The most likely reason why the modal description was not developed and the ideas by Peregrine & Smith (1975) and Peregrine (1976) were effectively abandoned is that it is not easy to construct the modes: in the linear limit one has to solve a two-dimensional boundary value problem with variable coefficients. Our work tackles this difficulty: we have found a way to reduce the original two-dimensional boundary value problem to a one-dimensional problem by using an asymptotic procedure under reasonably mild and geophysically relevant assumptions. This key finding provides the foundation for a systematic weakly nonlinear theory of wave dynamics on jet currents which will be considered elsewhere.

The work is organized as follows. In § 2 the problem of waves propagating on parallel jet currents is formulated in the linear setting. In § 3, exploiting the natural small parameters, current magnitude to wave celerity and wavelength to current width,

https://doi.org/10.1017/jfm.2013.584 Published online by Cambridge University Press

we develop an asymptotic approach to solving the two-dimensional boundary value problem. We utilize an asymptotic separation of variables that enables us to find a solution in terms of an asymptotic series in either of the two parameters. We show that for a wide range of parameters, the system of eigenfunctions forms a complete set if both the trapped modes corresponding to the discrete spectrum and the non-trapped modes corresponding to the continuous spectrum are taken into account. We focus our attention on the trapped waves. Properties of the trapped modes on currents are analysed in § 4 analytically (for model current profiles) and numerically. In § 5 we discuss the validation of the found asymptotic solutions by comparing them to numerical solutions. The results are summarized in § 6, where the key assumptions of the approach are discussed along with estimates for a variety of jet currents in nature.

2. Statement of the problem

We consider wave motions on the free surface of an ideal incompressible fluid of unit density. Waves are propagating on a given vertically uniform steady current $\boldsymbol{U}(x, y)$. The motions are governed by the standard Euler and continuity equations

$$\frac{\partial \boldsymbol{v}}{\partial t} + (\boldsymbol{U} + \boldsymbol{v}, \nabla)(\boldsymbol{U} + \boldsymbol{v}) + \nabla P = \boldsymbol{g}, \tag{2.1}$$

$$\nabla(\boldsymbol{U} + \boldsymbol{v}) = 0, \tag{2.2}$$

where $\boldsymbol{v}(x, y, z, t)$ is the fluid velocity with respect to the current $\boldsymbol{U}$, $P(x, y, z, t)$ is the pressure normalized by the water density, and $\boldsymbol{g}$ is the acceleration due to gravity. These governing equations are exact in the inviscid setting: no *a priori* assumptions on the nature of wave–current separation, the smallness of the wave motions or the structure of the current are required at this point.

To focus upon waves propagating on a jet-like current we first adopt the simplest possible model of a jet current: the current is assumed to be unidirectional, steady and vertically uniform. In the adopted Cartesian reference frame with the Ox axis parallel to the current and the Oz axis directed upward, the current velocity depends only on transverse coordinate y. For the chosen form of the current, $\boldsymbol{U} = (U(y), 0, 0)$, the continuity equation $\nabla(\boldsymbol{U} + \boldsymbol{v}) = 0$ gives the decoupled non-divergence condition on the velocity components of the wave field, $\boldsymbol{v} = (u, v, w)$:

$$\frac{\partial u}{\partial x} + \frac{\partial v}{\partial y} + \frac{\partial w}{\partial z} = 0. \tag{2.3}$$

The set of primitive equations (2.1) and (2.3) applies in the domain occupied by the fluid $-H \leqslant z \leqslant \eta$, where $H(x, y)$ is the water depth with respect to the water surface at rest and $\eta(x, y, t)$ is the water surface elevation. These equations are complemented by the standard boundary conditions. At the free surface, $z = \eta$, the pressure is assumed to be constant, and with no loss of generality may be set equal to zero,

$$P(x, y, z, t) = 0 \quad \text{at } z = \eta. \tag{2.4}$$

The standard kinematic condition on the water surface reads

$$\frac{\partial \eta}{\partial t} + (\boldsymbol{U} + \boldsymbol{v}, \nabla)\eta = w \quad \text{at } z = \eta. \tag{2.5}$$

The no-flux condition at the bottom, $z = -H(x, y)$, which we assume to be flat throughout the paper, requires

$$w = 0 \quad \text{at } z = -H. \tag{2.6}$$

https://doi.org/10.1017/jfm.2013.584 Published online by Cambridge University Press

On taking into account the assumed form of the current, we project the Euler equations (2.1) onto the chosen frame,

$$\left[\frac{\partial u}{\partial t} + U\frac{\partial u}{\partial x}\right] + (\boldsymbol{v}, \boldsymbol{\nabla})u + \frac{\partial U}{\partial y}v + \frac{\partial P}{\partial x} = 0, \tag{2.7a}$$

$$\left[\frac{\partial v}{\partial t} + U\frac{\partial v}{\partial x}\right] + (\boldsymbol{v}, \boldsymbol{\nabla})v + \frac{\partial P}{\partial y} = 0, \tag{2.7b}$$

$$\left[\frac{\partial w}{\partial t} + U\frac{\partial w}{\partial x}\right] + (\boldsymbol{v}, \boldsymbol{\nabla})w + \frac{\partial P}{\partial z} + g = 0. \tag{2.7c}$$

When supplemented by (2.3) and the kinematic boundary condition

$$\left[\frac{\partial \eta}{\partial t} + U\frac{\partial \eta}{\partial x}\right] + (\boldsymbol{v}, \boldsymbol{\nabla})\eta - w = 0 \quad \text{at } z = \eta, \tag{2.8}$$

and boundary conditions (2.4), (2.6), these equations constitute a closed system of equations and form the basis of our study. In this paper we confine our consideration to the linear setting, that is, we retain only the linear terms with the orbital velocity components u, v, w and the surface displacement η, which constitutes the subject of the classical linear theory (e.g. Phillips 1966; Peregrine 1976; Lighthill 2001).

3. Trapped modes: asymptotic expansion

Even within the framework of linear theory the trapped modes, in which we are primarily interested here, were examined for only a narrow class of situations and without developing a general asymptotic approach (see the review in Peregrine 1976). There is a large group of works based upon the WKB approach (e.g. Kenyon 1971) which assumes the transverse scale of the wave motion to be much smaller than the transverse scale of the current. This assumption automatically excludes low trapped modes. The main thrust of Peregrine & Smith (1975) was to consider the full two-dimensional boundary value problem. Inevitably such an approach was confined to a few tractable examples.

3.1. *The two-dimensional boundary value problem for trapped and free modes*

In this section we develop an asymptotic mathematical model of trapped waves on jet currents in the generic linear setting. Assuming uniformity of the problem with respect to x and t enables us to take the Fourier transform with respect to these variables and then to look for solutions in the form of superposition of travelling waves, propagating collinear to the current, with some lateral structure. Each harmonic constituent is characterized by its cyclic frequency, ω, and longitudinal wavenumber, k; k is assumed to be positive with no loss of generality. Thus we can use the following ansatz to describe the wave field components:

$$\eta(x, y, t) = A(y)\exp(\mathrm{i}\omega t - \mathrm{i}kx), \tag{3.1a}$$

$$u(x, y, z, t) = \hat{u}(y, z)\exp(\mathrm{i}\omega t - \mathrm{i}kx), \tag{3.1b}$$

$$v(x, y, z, t) = \hat{v}(y, z)\exp(\mathrm{i}\omega t - \mathrm{i}kx), \tag{3.1c}$$

$$w(x, y, z, t) = \hat{w}(y, z)\exp(\mathrm{i}\omega t - \mathrm{i}kx), \tag{3.1d}$$

$$P(x, y, z, t) = \hat{P}(y, z)\exp(\mathrm{i}\omega t - \mathrm{i}kx) - gz. \tag{3.1e}$$

https://doi.org/10.1017/jfm.2013.584 Published online by Cambridge University Press

Then the Euler equations (2.7*a*), (2.7*b*) and (2.7*c*) complemented by (2.3) and appropriate lateral boundary conditions, which we discuss later, yield the following boundary value problem on $\hat{w}(y,z)$:

$$\frac{\partial^2\hat{w}}{\partial z^2}+\frac{\partial^2\hat{w}}{\partial y^2}+\left(\frac{\Omega''}{\Omega}-2\frac{\Omega'^2}{\Omega^2}-k^2\right)\hat{w}=0 \quad \text{where } \Omega(y)\equiv\omega-kU. \tag{3.2}$$

Hereafter, $\partial_y f\equiv f'$.

Other components of the orbital velocity and pressure are expressed in terms of $\hat{w}$ as

$$\hat{u}(y,z)=\hat{u}(y,z_0)-\mathrm{i}\frac{\Omega'}{k\Omega}\int_{z_0}^{z}\frac{\partial\hat{w}(y,\xi)}{\partial y}\,\mathrm{d}\xi-\mathrm{i}k\left(1+\frac{\Omega'^2}{k^2\Omega^2}\right)\int_{z_0}^{z}\hat{w}(y,\xi)\,\mathrm{d}\xi, \tag{3.3a}$$

$$\hat{v}(y,z)=\hat{v}(y,z_0)+\int_{z_0}^{z}\frac{\partial\hat{w}(y,\xi)}{\partial y}\,\mathrm{d}\xi+\frac{\Omega'}{\Omega}\int_{z_0}^{z}\hat{w}(y,\xi)\,\mathrm{d}\xi, \tag{3.3b}$$

$$\hat{P}(y,z)=\hat{P}(y,z_0)-\mathrm{i}\Omega\int_{z_0}^{z}\hat{w}(y,\xi)\,\mathrm{d}\xi, \tag{3.3c}$$

where z_0 is an arbitrarily chosen reference depth level. The velocity fields and the pressure at the reference depth level $\hat{u}(z_0)$, $\hat{v}(z_0)$ and $\hat{P}(y,z_0)$ are constrained by (2.3) and (2.7).

Surface boundary condition (2.4), i.e. the requirement that $\hat{P}=0$ at $z=\eta$, specifies the integration constant in (3.3*c*), so that

$$\hat{P}(y,z)=gA-\mathrm{i}\Omega\int_{\eta}^{z}\hat{w}(y,\xi)\,\mathrm{d}\xi. \tag{3.4}$$

The linearized kinematic boundary condition on the water surface (2.8) relates the vertical velocity and the surface elevation amplitude

$$\mathrm{i}\Omega A=\hat{w} \quad \text{at } z=0. \tag{3.5}$$

The dynamic boundary condition on the water surface is automatically taken into account in (3.4). The pressure should remain constant on the water surface, and thus $\mathrm{d}P/\mathrm{d}t=0$, where the derivative is taken on the water surface. On applying this condition to (3.4) and linearizing it, we arrive at the relation in the form (see Mei, Stiassnie & Yue 2005, § 3.6)

$$\mathrm{i}\Omega\hat{P}=g\hat{w} \quad \text{at } z=0. \tag{3.6}$$

In combination with linearized (2.7*c*), this condition requires

$$\Omega^2\hat{w}=g\frac{\partial\hat{w}}{\partial z} \quad \text{at } z=0. \tag{3.7}$$

To find trapped and free modes for a given current profile $U(y)$, one has to solve the two-dimensional boundary value problem, which consists of the problem in the water bulk, (3.2), with boundary condition at the water surface (3.7), and at the bottom (2.6), and with solutions outside the jet, $y\to\pm\infty$, decaying to zero for the trapped modes and asymptotically approaching constant amplitude monochromatic waves for the free ones.

3.2. *Exact linear theory*

Solutions of boundary value problem (3.2) and (3.7) and the corresponding bottom and lateral boundary conditions specify wave modes $\hat{w}$ as functions of independent

https://doi.org/10.1017/jfm.2013.584 Published online by Cambridge University Press

variables y and z and parameters k and ω. It is easy to see that (3.2) admits separation of variables:

$$\hat{w}(y, z) = Y(y)Z(z). \tag{3.8}$$

Then the vertical and the lateral structure of the wave field are given by

$$\frac{\mathrm{d}^2 Z}{\mathrm{d}z^2} = h^2 Z, \tag{3.9a}$$

$$\frac{\partial^2 Y}{\partial y^2} + \left[\frac{\Omega''}{\Omega} - 2\frac{\Omega'^2}{\Omega^2} + h^2 - k^2\right] Y = 0, \tag{3.9b}$$

where h^2 is a separation constant. In this paper we do not consider the situations when $\Omega = 0$, which correspond to critical layers. Here we simply mention that for the critical layers to exist on the jet currents without a counter-current, waves have to propagate downstream with the celerity below the maximal current speed. For the same wave vector $\boldsymbol{k}$, such waves cannot coexist with the upstream-propagating neutral trapped modes in which we are primarily interested.

When the function $Y(y)$ is localized within an interval $y_1 \leqslant y \leqslant y_2$ (which may be infinite), (3.9*b*) with appropriate lateral boundary conditions represents the classical Sturm–Liouville problem if we consider h^2 to be its eigenvalue. Separation constant h^2 may be of any sign, although it should be real for the expression in square brackets in (3.9*b*) to be real and continuous.

By virtue of the properties of the Sturm–Liouville problem, the eigenfunctions of the boundary value problem on the infinite interval form a complete orthogonal set of functions, provided both kinds of eigenfunctions are considered: free waves (which do not decay as $y \to \pm\infty$ and correspond to the continuous spectrum) and trapped waves localized in y which correspond to the discrete spectrum (e.g. Drazin & Johnson 1989).

Thus any solution to the boundary value problem under consideration can be presented in the form

$$\hat{w} = \sum_n^{\infty} Y_n(y)Z_n(z), \tag{3.10}$$

where the summation should be understood as integration when the eigenvalue h_n^2 is in the continuous spectrum, Y_n is the solution to (3.9*b*) with the eigenvalue $h^2 = h_n^2$ and appropriate conditions at the infinity, while Z_n is the corresponding solution of (3.9*a*),

$$Z_n(z) = B_n \exp(h_n z) + C_n \exp(-h_n z), \tag{3.11}$$

and B_n and C_n are constants to be determined. For deep water constants C_n should be set equal to zero. For simplicity we assume hereafter that the water depth is infinite, i.e. $H \to \infty$.

The condition at the water surface (3.7) constrains the values of h and ω, resulting in

$$\Omega^2 = gh. \tag{3.12}$$

It is easy to see that condition (3.12) cannot hold since $\Omega = \Omega(y)$, while h was assumed to be constant. This means that it is impossible to satisfy the boundary conditions separately for each mode $Y_n Z_n$.

In principle, the two-dimensional boundary value problem which consists of (3.2) and (3.7), the condition at the bottom and appropriate lateral conditions may be

https://doi.org/10.1017/jfm.2013.584 Published online by Cambridge University Press

analysed numerically. Aiming at an analytic description, in the next section we develop an asymptotic approach exploiting the slow dependence of h on y occurring in nature in most situations of interest. It allows us to reduce the challenging two-dimensional boundary value problem to a tractable problem. A numerical approach developed in appendix E is then used to validate the asymptotic theory in § 5.

3.3. *Asymptotic expansion for 'weak' and/or 'broad' currents*

In the oceanic context, the problem of waves on currents – the prime motivation of this study – usually contains natural small parameters that we have not yet exploited. The currents can be characterized by two independent dimensional parameters: the magnitude of the current, $|U_{max}|$, and its lateral scale, L. The basic parameters of the wave field with already chosen longitudinal wavenumber k having the same dimensions are the wave phase velocity C and the inverse longitudinal wavenumber k^{-1}. Often the typical wavelengths are much smaller than the lateral scale of the currents, which gives rise to a small parameter $\mu = (kL)^{-1}$ with typical values being $O(10^{-3}$–$10^{-2})$. The situations with $\mu \sim 10^{-1}$–10^{0} are also possible: they occur on quite narrow rip and longshore currents. When $\mu \ll 1$, which is common, we will introduce the notion of '*broad*' currents.

At the same time, as a rule, celerities C of the dominant wind waves and swell in the ocean far exceed the maximal speed of the currents U_{max}, which enables us to introduce and exploit a new small parameter $\gamma = |U_{max}/C| \ll 1$. Typically $\gamma \sim O(10^{-2}$–$10^{-1})$. When $\gamma \ll 1$ we will refer to such situations as '*weak*' currents.

Below we consider the situations both with small and order-one γ and μ. Crucially, as we show below, the smallness of either γ or μ causes the waves to be locally close to the solution for the uniform current; more specifically, it makes $h(y)$ a slow function of y. This fact enables us to develop a systematic asymptotic approach which we present in this section.

Without loss of generality the asymptotic solution to the initial problem can be sought in the form of a superposition of lateral modes with summation over the discrete spectrum of trapped modes and integration over free continuous spectrum modes. In this paper we focus on the neutral trapped modes, i.e. the modes with real eigenvalues which are the key basic elements of the scheme. To find asymptotically separable solutions we assume the vertical component of the velocity to be given by

$$\hat{w} = \sum_n B_n Y_n(y) Z_n(z, y), \tag{3.13}$$

where Z_n are now slow functions of y; the particular smallness will become apparent later on and justified *a posteriori*.

First we have to construct individual modes satisfying the equations and the boundary conditions. Each of these modes could be viewed as a self-contained object; the evolution of individual modes represents a meaningful physical problem of independent interest. Their study is necessary for the description of generic wave fields. It is expected that often the main part of a generic wave field can be captured by a finite, and sometimes relatively small, number of modal functions $Y_n(y)Z_n(z, y)$.

According to (3.11), the vertical mode $Z_n(z, y)$ for the deep water case is assumed to be close to an exponential function. We introduce the following ansatz (the underlying reasoning is given in appendix A):

$$Z_n(z, y) = [1 + z^2 f_n(z, y)]\overline{Z}_n(z, y), \quad \overline{Z}_n \equiv \exp(h_n(y)z). \tag{3.14}$$

https://doi.org/10.1017/jfm.2013.584 Published online by Cambridge University Press

In what follows, the auxiliary smooth functions f_n will be sought in the form of the Taylor expansion around $z = 0$. Note that $(\partial/\partial z)(z^2 f_n)$ vanishes as $z \to 0$ for any f_n, hence the auxiliary functions f_n do not affect the free surface boundary condition. Assuming $|f_n| \ll 1$ and $h_n(y, z)$ to be slow functions of y, functions h_n may be sought in the form of asymptotic series. Then boundary value problem (3.2) and (3.7) with appropriate lateral boundary conditions may be solved, once the physical small parameter ensuring the required slowness in y is identified. In this way we will effectively separate variables in (3.2) and hence reduce the two-dimensional boundary value problem to a one-dimensional problem for two important cases, of 'weak' and of 'broad' currents.

3.3.1. *'Weak' currents*

One of the most natural ways to develop an asymptotic procedure is to consider the typical situation where waves are propagating much faster than the current. Weakness of the current characterized by the already introduced small parameter γ results in a slow transverse variation of modes with the scale characterized by a new small parameter, $\chi \ll 1$. Formal definition of χ is given below by (3.17). Then, the asymptotic series for the mode eigenfrequency, ω_n, the counterpart of the separation constant h_n and eigenmode $\hat{w}_n$, may be constructed in the form

$$\omega_n = \omega_n^{(0)} + \chi^2 \omega_n^{(1)} + \chi^4 \omega_n^{(2)} + \cdots, \tag{3.15a}$$

$$h_n = h_n^{(0)} + \chi^2 h_n^{(1)} + \chi^4 h_n^{(2)} + \cdots, \tag{3.15b}$$

$$\hat{w}_n = \hat{w}_n^{(0)} + \chi \hat{w}_n^{(1)} + \chi^2 \hat{w}_n^{(2)} + \chi^3 \hat{w}_n^{(3)} + \chi^4 \hat{w}_n^{(4)} + \cdots. \tag{3.15c}$$

More precisely, in agreement with (3.14) the vertical velocities may be sought in the form

$$\hat{w}_n^{(0)} = B_n^{(0)} Y_n^{(0)} \overline{Z}_n, \tag{3.16a}$$

$$\hat{w}_n^{(1)} = B_n^{(1)} Y_n^{(1)} \overline{Z}_n, \tag{3.16b}$$

$$\hat{w}_n^{(2)} = B_n^{(2)} (Y_n^{(2)} + z^2 Y_n^{(22)}) \overline{Z}_n, \tag{3.16c}$$

$$\hat{w}_n^{(3)} = B_n^{(3)} (Y_n^{(3)} + z^2 Y_n^{(32)}) \overline{Z}_n, \tag{3.16d}$$

$$\hat{w}_n^{(4)} = B_n^{(4)} (Y_n^{(4)} + z^2 Y_n^{(42)} + z^3 Y_n^{(43)} + z^4 Y_n^{(44)}) \overline{Z}_n, \tag{3.16e}$$

$$\overline{Z}_n = \exp(h_n z). \tag{3.16f}$$

Functions $Y_n^{(22)}$, $Y_n^{(32)}$, $Y_n^{(42)}$, $Y_n^{(43)}$ and $Y_n^{(44)}$ are auxiliary functions of y to be specified by compatibility conditions. All modal functions $Y_n^{(\ldots)}$ in (3.16) are assumed to be slow functions of y:

$$\chi \sim \frac{\partial Y_n^{(\ldots)}/\partial y}{k Y_n^{(\ldots)}}. \tag{3.17}$$

Here χ is the mode characteristic non-dimensional inverse transverse scale, a generalization of the non-dimensional characteristic transverse wavenumber, or, more accurately, the local transverse wavenumber normalized by the longitudinal one. Note that χ is not the characteristic inverse lateral size of the mode $Y(y)$. For modes trapped by weak currents, the parameter χ is related to γ as $\chi^2 \sim \gamma$; this relation will be discussed below.

Consideration of the basic system of (3.2) and (3.7) at different orders of χ allows us to solve the problem asymptotically. Condition (3.7) specifies h_n as a function of k and ω_n. Condition (3.2) links k and ω_n and specifies lateral mode dependence. In this section we provide just a brief outline of the asymptotic expansion and discuss the

https://doi.org/10.1017/jfm.2013.584 Published online by Cambridge University Press

main results. In what follows, the slow coordinates are not explicitly indicated. Further details of the multiple-scale asymptotic derivation are given in appendix B.

To leading order, $O(\chi^0)$, the waves are deep water surface waves propagating strictly against the current and unaffected by the current; relations (3.2) and (3.7) give the classical dispersion relation for free waves,

$$h^{(0)} = k, \quad gk = \omega^{(0)2}, \tag{3.18}$$

where subscript n is omitted hereafter.

To order $O(\chi^1)$, no new terms appear in the dispersion relation. Order $O(\chi^2)$ results in the following correction to the dispersion relation:

$$h^{(1)}(y) = 2k\frac{\Omega^{(1)}}{\omega^{(0)}} \quad \text{where } \Omega^{(1)} \equiv \omega^{(1)} - kU(y). \tag{3.19}$$

Note that although the transverse derivative of $Y^{(0)}$ with respect to y is of order χ, the transverse derivative of $\overline{Z}_n$ is of order χ^2; thus the vertical mode function is characterized by a $O(\chi)$ slower lateral dependence. It is also easy to see that $\partial h/\partial y$ is $O(\chi^2) \sim \gamma$.

To this order the boundary value problem for trapped modes takes the form

$$\widehat{L}_\gamma Y^{(0)} = 0 \quad \text{where } \widehat{L}_\gamma Y \equiv \frac{\partial^2 Y}{\partial y^2} + \frac{4k^2}{\omega^{(0)}}[\omega^{(1)} - kU]Y, \tag{3.20}$$

and

$$Y^{(0)}(y) \to 0 \quad \text{as } y \to \pm\infty. \tag{3.21}$$

The boundary value problem (3.20) provides an extra *a posteriori* justification for the previously mentioned relation between small parameters: $\chi \sim \gamma^{1/2}$. Note that derivatives of U do not enter the boundary value problem (3.20), hence it is valid for any value of μ as long as $\gamma \ll 1$.

The $O(\chi^3)$ and $O(\chi^4)$ terms in the expansion are derived in appendix B. Higher-order asymptotic terms may be obtained in a similar fashion, although the derivation becomes rather tedious. In this paper we focus on the leading-order problem for trapped modes (3.20), which will be discussed in detail in § 4.

3.3.2. *'Broad' currents*

Consideration of 'broad' currents specified by the requirement $\mu \ll 1$ enables us to construct an alternative asymptotic scheme to tackle (3.2) and (3.7) without the weak current assumption. To this end we treat U and h_n as slow functions of y with the slowness prescribed by the broad current small parameter μ, i.e. $U = U(\mu y)$ and $h_n = h_n(\mu y)$. Then the asymptotic series for wave frequency and vertical velocity component may be written in the form

$$\omega_n = \omega_n^{(0)} + \mu\omega_n^{(1)} + \mu^2\omega_n^{(2)} + \cdots, \tag{3.22a}$$

$$h_n = h_n^{(0)} + \mu h_n^{(1)} + \mu^2 h_n^{(2)} + \cdots, \tag{3.22b}$$

$$\hat{w}_n = \hat{w}_n^{(0)} + \mu\hat{w}_n^{(1)} + \mu^2\hat{w}_n^{(2)} + \cdots. \tag{3.22c}$$

Parameter γ is now assumed to be of order one; hence, strong currents can be considered if necessary. The expansion in μ explicitly depends on γ. The small γ limit of the theory will be considered in § 4.2. We stress that smallness of μ is not equivalent to the WKB approximation; this point is discussed separately below.

https://doi.org/10.1017/jfm.2013.584 Published online by Cambridge University Press

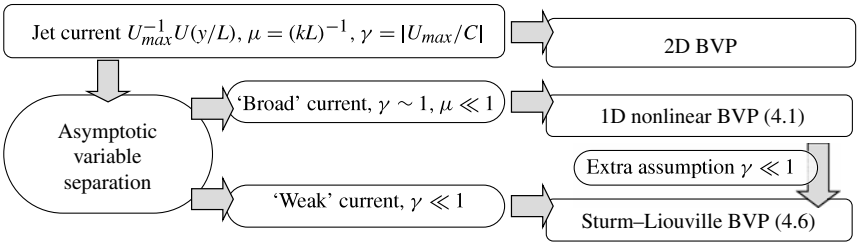


FIGURE 1. A sketch illustrating the developed asymptotic theory based on the approximate separation of variables. See discussion in § 6.1.

In accordance with (3.14) we assume the following ansatz for vertical velocities:

$$\hat{w}_n^{(0)} = B_n^{(0)} Y_n^{(0)} \overline{Z}_n, \tag{3.23a}$$

$$\hat{w}_n^{(1)} = B_n^{(1)} (Y_n^{(1)} + z^2 Y_n^{(12)}) \overline{Z}_n, \tag{3.23b}$$

$$\hat{w}_n^{(2)} = B_n^{(2)} (Y_n^{(2)} + z^2 Y_n^{(22)} + z^3 Y_n^{(23)} + z^4 Y_n^{(24)}) \overline{Z}_n, \tag{3.23c}$$

$$\overline{Z}_n = \exp(h_n z). \tag{3.23d}$$

Details of the derivation of both the leading-order and the next-order solution are given in appendix B.

To leading order $O(\mu^0)$, we get the generalized dispersion relation

$$g h^{(0)}(y) = \Omega^{(0)^2} \quad \text{where } \Omega^{(0)} \equiv \omega^{(0)} - kU(y). \tag{3.24}$$

The boundary value problem for trapped modes reads

$$\widehat{L}_\mu Y^{(0)} = 0, \quad Y(y) \to 0 \quad \text{as } y \to \pm\infty \text{ where } \widehat{L}_\mu Y \equiv \frac{\partial^2 Y}{\partial y^2} + [h^{(0)^2} - k^2] Y, \tag{3.25}$$

where subscript n is omitted for brevity. Note that for strong currents the leading-order eigenfrequency, $\omega^{(0)}$, may differ significantly from the frequency of freely propagating waves.

The compatibility condition (3.12) remains approximately valid for ansatz (3.13); it specifies a slowly varying quantity $\Omega^{(0)}(y) = \omega^{(0)} - kU$, which is an analogue of intrinsic frequency. By virtue of (3.24), $\Omega^{(0)}$ is directly linked to the slow function $h^{(0)}$; the slowness is specified by the estimates $\mathrm{d}h^{(0)}/\mathrm{d}y \sim k^2\gamma\mu$ and $\mathrm{d}^2h/\mathrm{d}y^2 \sim k^3\gamma\mu^2$.

The extension of this asymptotic expansion to higher orders may be obtained in a similar way. The procedure and results for the next order are given in appendix B.

4. The leading-order boundary value problem for weak currents

In the previous section we outlined a way to separate the variables in (3.2) asymptotically into horizontal and vertical modes, which allows us to avoid solving the original two-dimensional boundary value problem head-on. Two different families of approximate one-dimensional problems have been obtained, as shown schematically in figure 1. In this section we discuss their properties and interrelations.

4.1. *'Broad' currents*

Under the broad current assumption, allowing the current to be strong, the horizontal modes are specified to leading order in μ by the following boundary value problem

https://doi.org/10.1017/jfm.2013.584 Published online by Cambridge University Press

on Y, which does not depend on z:

$$\frac{\partial^2 Y}{\partial y^2} + \left[\frac{\Omega^4}{g^2} - k^2\right] Y = O(\mu). \tag{4.1}$$

As in the previous section, the boundary condition $Y(y) \to 0$ as $y \to \pm\infty$ selects the trapped modes; more general non-vanishing conditions

$$Y(y) \to C_1 \exp(-\mathrm{i}qy) + C_2 \exp(\mathrm{i}qy) \quad \text{at } y \to +\infty, \tag{4.2a}$$

$$Y(y) \to C_3 \exp(-\mathrm{i}qy) + C_4 \exp(\mathrm{i}qy) \quad \text{at } y \to -\infty, \tag{4.2b}$$

where C_i, $i = 1, 2, 3, 4$ are constants and q is a real constant, specify free modes. Free modes are not considered in the present work: we confine our attention to the boundary value problem (4.1) with vanishing boundary conditions, where frequency ω_n, hidden in $\Omega_n = \omega_n - kU(y)$, plays the role of the eigenvalue.

The vertical modes corresponding to the nth eigenvalue are specified by

$$Z_n = \exp(h_n(y)z), \quad h_n(y) = \frac{\Omega_n^2}{g} = \frac{(\omega_n - kU(y))^2}{g}. \tag{4.3}$$

We emphasize that $Z(y, z)$ is a slow function of y by virtue of the slowness of $h(y)$. We also note that to leading order in μ, the boundary value problem (4.1) with the right-hand side set to be zero does not explicitly depend on smallness of μ.

The as yet unspecified frequency ω enters into (4.1) via the quantity Ω. It is straightforward to show that only one eigenfunction of (4.1) corresponds to each value of ω for a given k, if the condition $YY' \to 0$ as $y \to \pm\infty$ is satisfied. The situation is more complicated for more general boundary conditions. Indeed, assume that there are two different functions Y_1 and Y_2 that correspond to the same eigenfrequency, ω and k. Then, by virtue of (4.1), it is easy to see that

$$Y_1'' Y_2 - Y_1 Y_2'' = 0. \tag{4.4}$$

Then the quantity $Y_1'' Y_2 - Y_1 Y_2''$ may be integrated once, which yields

$$\frac{\mathrm{d}}{\mathrm{d}y}(Y_1/Y_2) = \text{const}. \tag{4.5}$$

For free modes the constant is not necessarily zero and there is a double degeneracy of the eigenvalues. For the trapped modes vanishing at infinity the constant is zero, which immediately yields $Y_1 = \text{const.} \times Y_2$, i.e. the eigenfunctions of the trapped modes are linearly dependent (see Landau & Lifshitz 1977, § 21). Because (4.1) is a second-order linear differential equation and in the case of free modes both of the two linearly independent solutions are non-zero and may satisfy the boundary conditions (4.2), two modes of passing-through waves correspond to one pair of k and ω.

In this paper we concentrate on the analysis of the leading-order boundary value problem (4.1) for trapped modes. It is straightforward to solve (4.1) numerically, while to progress analytically, additional approximations are required.

4.2. *Reduction to Sturm–Liouville type*

An inconvenient feature of the leading-order boundary value problem (4.1) is that the eigenvalue ω enters (4.1) in a nonlinear fashion via $\Omega = \omega - kU$. To arrive at the classical form of the eigenvalue problem, we can utilize the relative smallness of the speed of the current with respect to wave celerity characterized by the previously introduced small parameter γ. So far we have not used smallness of γ, allowing it

https://doi.org/10.1017/jfm.2013.584 Published online by Cambridge University Press

to be $O(1)$ in (4.1). On expanding the square brackets in (4.1) in the Taylor series in γ and then retaining the leading-order terms, we reduce (4.1) to the much simpler boundary value problem of Sturm–Liouville type,

$$\frac{\partial^2 Y}{\partial y^2} - \left[4\frac{k^3 U}{\sqrt{kg}} + l^2\right] Y = O(\gamma^2, \mu), \quad Y(y) \to 0 \quad \text{as } y \to \pm\infty, \tag{4.6}$$

where the quantity $l^2 \equiv k^2 - \omega^4/g^2$ could now be treated as the eigenvalue of (4.6).

Value l^2 is assumed to be small. Indeed, trapped modes may exist when l^2 is of the order of the current velocity, i.e. $l^2 \sim \gamma$. As a result, ω enters into the problem only through the introduced parameter l^2:

$$\omega = \sqrt[4]{g^2(k^2 - l^2)}. \tag{4.7}$$

For small l, (4.7) reduces to $\omega = \sqrt{kg}(1 - l^2/(4k^2))$.

Note that (4.6) coincides with the leading-order in γ boundary value problem for trapped waves (3.20) upon setting $\omega^{(1)} = -\sqrt{gk}l^2/k^2$, which is equivalent to relabelling the eigenvalue. Recall that (3.20) has been derived to $O(\chi^4) \sim O(\gamma^2)$ accuracy without assumptions regarding broadness of the current. In the limit of small γ the second-order terms of the expansion in μ vanish. Indeed, by virtue of (B 18), $Y^{(12)} \sim \partial Y^{(0)}/\partial y\, \partial h^{(0)}/\partial y_\mu \sim \gamma\mu\chi$, where $\chi \sim \sqrt{\gamma}$ for small γ. As a result, $\omega^{(1)}$ and $Y^{(1)}$ are proportional to $\gamma^{3/2}$ as well, and hence vanish when $\gamma \to 0$. Hence the accuracy of (4.6) is underestimated. Various mixed terms due to two small parameters, γ and μ, appear in the higher asymptotic orders of the γ and μ expansions: see the details in appendix B. Strictly speaking, for (3.20) to be the true small γ limit of the expansion in μ (3.22), not only the second-order terms of the expansion in μ but also all high-order terms have to vanish when $\gamma \to 0$. This vanishing remains a conjecture.

Waves propagating against the current, i.e. with $kU < 0$, can be trapped by the jet current; for such waves $l^2 > 0$. A boundary value problem similar to (4.6) was obtained by Peregrine & Smith (1975) as the local limit solution for low mode-number waves.

Trapped modes exist owing to the balance between the terms in (4.6). We reiterate that the spatial scale of the eigenfunctions depends on the shape of the current. A rough estimate of the characteristic gradient of a mode in the transverse direction yields $\chi \sim \gamma^{1/2}$. In the general case the spatial scale of the jet current, $k^{-1}\mu^{-1}$, and of trapped modes, $k^{-1}\chi^{-1}$, do not coincide, since γ and μ are physically unrelated parameters.

Recall that by retaining higher-order terms in the expansion in γ in (4.1), we obtain a sequence of boundary value problems with higher accuracy, the price being nonlinear dependence on the eigenvalue parameter. Thus all these higher-order boundary value problems are not of Sturm–Liouville type, although, as we show in appendix D, they are in a certain sense close. We now focus upon the basic properties of the Sturm–Liouville model (4.6).

4.3. *Basic properties of the Sturm–Liouville-type boundary value problem*

Boundary value problem (4.6) has the form of the classical stationary Schrödinger equation (see e.g. Landau & Lifshitz 1977; Drazin & Johnson 1989). The eigenmodes of (4.6) with generic, i.e. either decaying or non-vanishing, boundary conditions on an infinite line, that is, those corresponding to both trapped and passing-through free wave modes, constitute a complete set of functions which correspond to the discrete and continuous spectrum of eigenvalues. Therefore any wave field over the current

https://doi.org/10.1017/jfm.2013.584 Published online by Cambridge University Press

may be uniquely represented by a combination of trapped and free wave modes. An exception requiring special consideration is the situations when the critical layers are present, i.e. there are points where $\Omega = \omega - kU(y) = 0$.

Trapped modes correspond to discrete eigenvalues $l^2 > 0$. If for the chosen wavenumber k, $kU < 0$, then at least one localized solution of (4.6) always exists (e.g. Simon 1976; Landau & Lifshitz 1977). If kU is not sign-definite, that is, for currents with counter-currents, the situation requires special consideration. However, for the 'shallow well' situations, that is, for $|U_{max}|/\sqrt{g/k}(kL)^2 \ll 1$, or, in terms of non-dimensional parameters, $\gamma \ll \mu^2$, condition $\int_{-\infty}^{\infty} kU\,\mathrm{d}y \leqslant 0$ is the necessary and sufficient criterion for the existence of trapped modes (Simon 1976).

A number of exact solutions for the stationary Schrödinger equation (4.6) for particular profiles of the well has been known for several decades: see e.g. Landau & Lifshitz (1977). Four examples which are simple and, at the same time, capture the main properties of the trapped modes on currents are discussed in appendix C. These model profiles include: (i) a 'top-hat' current ($U = U_m = \text{const.}$ for $|y| < L$, $U = 0$ for $|y| > L$); (ii) a parabolic current ($U = ay^2 + b$, where a and b are constants); (iii) a sech-squared shape ($U = U_0\,\mathrm{sech}^2(y/L)$); (iv) a asymmetric triangular profile ($U = ay$ for $-L < y < 0$, where a is a constant, and $U = 0$ elsewhere).

Our approach could be briefly summarized as follows. Due to the uniformity of the problem with respect to x and t, the solution of the system of exact linear equations allows a mode representation, where the modes are functions of the transverse and vertical coordinates satisfying problem (3.2) and (3.7). Under only the assumption of a slow lateral dependence of the current, $\mu \ll 1$, the separation of horizontal and vertical modes takes place, according to (3.13) and (4.1) via the separation variable h, which is a slow function of the transverse coordinate.

The boundary value problem on trapped waves (4.1) is of a non-classical kind, and at first glance looks too complicated for substantial analytical progress. On making use of the natural smallness of current relative magnitude, $\gamma \ll 1$, to leading order in γ the problem reduces to the Sturm–Liouville eigenvalue problem in the form of the stationary Schrödinger equation (4.6). We can arrive at the same Sturm–Liouville problem (4.6) only with the assumption of a weak current, $\gamma \ll 1$, for $\mu \sim 1$ as well: see figure 1. One of the main advantages of the Sturm–Liouville problem (4.6) is the orthogonality and completeness of the set of eigenmodes comprising both the free and trapped modes.

The proximity of modes of the boundary value problem (4.1) for non-small γ to the eigenfunctions of the small γ boundary value problem (4.6) and significance of non-orthogonality of eigenfunctions of (4.1) is examined in appendix D in the general case. It has been shown that for relatively low modes (4.1) could be reduced to the Sturm–Liouville problem. The accuracy of such an asymptotic reduction has been tested in appendix D for particular examples of parabolic currents with γ up to about $\gamma \approx 0.5$. It is found that even for such order-one γ the low modes exhibit excellent one-to-one correspondence between the solutions of the exact in γ boundary value problem (4.1) and its small γ approximation (4.6) as long as μ remains sufficiently small. Approximate orthogonality of modes of (4.1) was found to hold well for non-small γ. A comparison of dispersion relations for trapped modes prescribed by the boundary value problems (4.6) and (4.1) is discussed below and illustrated in figure 2(*d*). Remarkably, the solutions of the small γ boundary value problem (4.6) proved to be quantitatively very good even for rather strong currents.

https://doi.org/10.1017/jfm.2013.584 Published online by Cambridge University Press

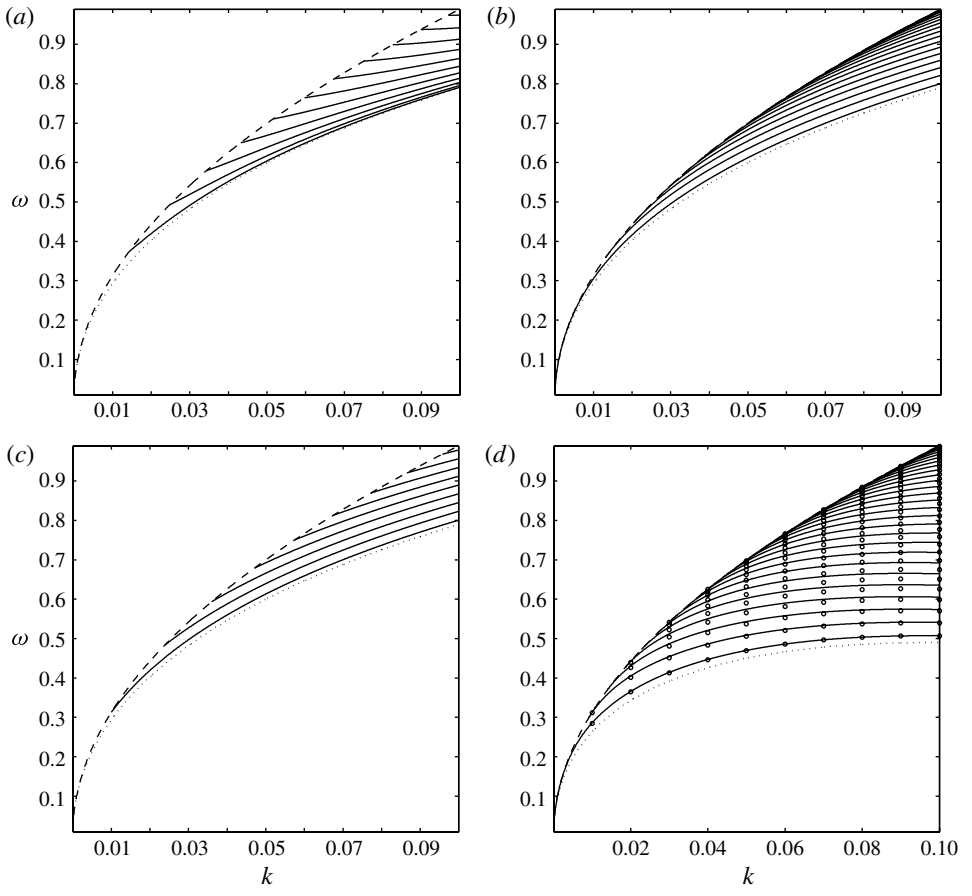


FIGURE 2. The dispersion relation for trapped waves on model currents (4.11) linking ω in rad s^{-1} and the longitudinal wavenumber k in rad m^{-1} (solid lines): (*a*) a top-hat current (the limit of a 'deep potential well'), $U_m = -2$ m s^{-1}, $L = 200$ m; (*b*) a sech-squared shape current with $U_0 = -2$ m s^{-1}, $L = 200$ m; (*c*) a parabolic current with $U(0) = -2$ m s^{-1}, $L = 200$ m. (*d*) Similar relations for a sech-squared current with $U_0 = -5$ m s^{-1}, $L = 200$ m: the approximate solution (4.11) (lines) and the numerical solution of the boundary value problem for broad currents (4.1) (circles). Two envelopes of the family of the dispersion curves are also shown: the outer envelope is the deep water surface gravity wave dispersion curve $\omega = \sqrt{kg}$, plotted by the dashed line; the inner envelope is $\omega = \sqrt{kg} + kU_{max}$, shown by the dotted line.

4.4. *Number of trapped modes and the scale of mode localization*

The number of trapped modes supported by a given current $U(y)$ within the framework of the small γ boundary value problem (4.6) can be estimated by employing the WKB or semi-classical approximation (e.g. Landau & Lifshitz 1977, § 48). Then the Bohr–Sommerfeld quantization rule gives the following estimate for the number of trapped modes, N_{tr};

$$N_{tr} = \frac{2k}{\pi\sqrt[4]{kg}} \int_{-\infty}^{\infty} \sqrt{-kU(y)}\,\mathrm{d}y + \frac{1}{2} \approx \frac{2k}{\pi} \int_{-\infty}^{\infty} \sqrt{-\frac{U}{C}}\,\mathrm{d}y + \frac{1}{2}, \tag{4.8}$$

https://doi.org/10.1017/jfm.2013.584 Published online by Cambridge University Press

where $C = \omega/k$. Strictly speaking, this formula is valid only for a large number of trapped modes, though it often gives a reasonable estimate even when this number is small. An idea of the accuracy of (4.8) for a low number of modes can be grasped by comparing the threshold in the current magnitude when new modes emerge according to (4.8) and its true value. For the example of a sech-shape current considered in § C.2 for which solutions are known, and one mode always exists, the error in the threshold value of the current magnitude is ∼12.5 % for $N_{tr} = 2$, and 4 and 2 %, respectively, for $N_{tr} = 3, 4$. Estimates of N_{tr} for various currents will be discussed separately below.

Note that the number of trapped modes N_{tr}, an important integral characteristic of the current, can be explicitly expressed in terms of basic independent small parameters γ and μ according to (4.8):

$$N_{tr} \sim \sqrt{\gamma}/\mu. \tag{4.9}$$

In the fairly common regime characterized by $N_{tr} \gg 1$, a simple analytic solution obtained for the parabolic current (C 10) provides a good asymptotic approximation for the description of low modes, i.e. with $n \sim 1$; then the transverse wavenumber can be estimated as $k_y^2 \sim k^2 n\sqrt{\gamma}\mu$. It is illuminating to express the characteristic transverse scale for the nth mode, $\chi \sim k_y/k$, in terms of n and N_{tr}. It is easy to see that $\chi \sim \sqrt{\gamma}\,(n/N_{tr})^{1/2}$. Hence, for $n \sim 1$ the dependence on n can be neglected and the scale in terms of N_{tr} can be expressed in the ultimately simple way $\chi \sim \sqrt{\gamma/N_{tr}}$. In the general case $\chi \lesssim \sqrt{\gamma}$.

The overall transverse scale of the nth mode $nk^{-1}\chi^{-1}$ can be easily estimated:

$$nk^{-1}\chi^{-1} \sim \frac{1}{k}\sqrt{nN_{tr}/\gamma} \approx \frac{1}{k}\sqrt{\frac{n}{N_{tr}}}\sqrt{N_{tr}^2/\gamma} \approx \frac{1}{k\mu}\sqrt{\frac{n}{N_{tr}}}. \tag{4.10}$$

Thus, the scale of the nth mode localization is a $\sqrt{n/N_{tr}}$ fraction of the transverse scale of current L; for $N_{tr} \gg 1$ the low modes are confined to a narrow vicinity of the maximum of the current.

4.5. *Dispersion relation*

Once the eigenvalues l_n are found by solving the boundary value problem (4.6), then the dispersion relation as a function of $\omega_n(k)$ is given by (4.7). Note that a number of frequencies $\omega_n(k)$ correspond to each value of longitudinal wavenumber k, the number being dependent on k: for low k there is a single mode while in the limit of large k the number tends to N_{tr} given by (4.8). Making further use of the smallness of l^2 compared to k, it is possible to cast the dispersion relation (4.7) in several asymptotically equivalent representations. The presentation

$$\omega_n = \sqrt{gk}\left(1 - \frac{1}{4}\frac{l^2}{k^2}\right) \tag{4.11}$$

makes it particularly easy to see that the eigenfrequencies $\omega_n(k)$ are bounded above by the classical deep water dispersion relation $\omega = \sqrt{kg}$, which corresponds to $l^2 = 0$. The lower bound is not obvious from this form; the lower bound is given by the dispersion relation for waves on the uniform current $\omega = \sqrt{kg} + kU_{max}$ with $kU_{max} < 0$, where the value of $|U_{max}|$ corresponds to the maximum of current velocity. Representation (4.11) is also consistent with the asymptotic theory for ω_n for small γ and $\mu \sim 1$: see (3.20).

Dispersion relation (4.11) for three sample model profiles is plotted in figure 2(*a–c*) (solid lines). For illustrative convenience the plots are made for the case of a very strong and narrow jet current with parameters possible for rip currents. The sample

https://doi.org/10.1017/jfm.2013.584 Published online by Cambridge University Press

model profiles are the top-hat, sech-squared and parabolic. The thick dashed lines indicate the classical deep water dispersion relation, while the dotted lines correspond to $\omega = \sqrt{kg} + kU_{max}$. Note that the top-hat model in the limit of a 'deep potential well' is not valid for long waves. The parabolic current does not vanish at infinity, and thus only the low-mode exact solutions out of infinitely many trapped modes in this model are likely to describe the reality. Therefore the plots in figure 2(*a*,*c*) are designed to demonstrate only basic generic qualitative features of the trapped mode dispersion relation. Indeed, very different profiles yield a qualitatively similar $\omega(k)$ behaviour of the trapped modes.

The number of trapped modes increases with the increase of k. A new trapped mode appears for wavenumbers exceeding a 'cut-off' value k^* specified by the condition $l_n^2 = 0$. The 'cut-off' wavenumber k^* depends on the shape of the current. For example, for a parabolic current the cut-off wavenumber for the nth mode is given by the following explicit expression:

$$k^* = \frac{gU''^2}{64U(0)^2}(2n+1)^2, \quad n = 0, 1, \ldots. \tag{4.12}$$

The distribution of density of trapped modes' eigenfrequencies ω for a given k also depends on the shape of the jet current.

The dispersion curves discussed above and plotted in figure 2(*a–c*) were obtained within the framework of the Sturm–Liouville boundary value problem (4.6) under assumption $\gamma \ll 1$. To get an idea of how important this approximation is, in figure 2(*d*) we compare the approximate analytic solution for a sech-squared current with a numerical solution of the boundary value problem (4.1) for the case of an extraordinarily strong current. Even for this extreme case, the agreement between the approximate analytic solution (solid curves) and the results of the numerical solution of the exact in γ boundary value problem (4.1) shown by circles is very good. The observation enables us to use the Sturm–Liouville approximate results beyond the domain of their asymptotic validity, at least for the qualitative description of trapped modes. Analytical and numerical justifications of such a proximity are discussed in appendix D.

Although it is not apparent from the plots in figure 2, the group velocity and especially its derivative $\mathrm{d}^2\omega/\mathrm{d}k^2$ are smaller for trapped modes than for collinear free waves. Provided γ is no longer small, $\mathrm{d}^2\omega/\mathrm{d}k^2$ changes sign for sufficiently high mode numbers, i.e. dispersion relation $\omega_n(k)$ might have an inflection point. It is easy to see the emergence of an inflection point for the example of a top-hat current of width L: for $\mathrm{d}^2\omega/\mathrm{d}k^2 \sim -4(kL)^2 + 15\pi^2 n^2$, there is an inflection point for $n \sim kL/(2\pi)$. Similar results could be obtained for other shapes of the current. For lower mode numbers and weaker currents there are no inflection points, and yet there is always a $O(\gamma)$ decrease of $\mathrm{d}^2\omega/\mathrm{d}k^2$, which is expected to have important implications for the nonlinear evolution of narrow-band wave fields.

5. Numerical validation of the asymptotic solutions for trapped modes

The original two-dimensional boundary value problem consists of the equation in the water bulk (3.2) complemented by the surface condition (3.7) and appropriate conditions at the bottom, and far from the current. To tackle the problem we have employed approximate separation of variables by introducing slow functions $h_n(y)$. An essential element of the approach is that the surface boundary condition (3.7) is satisfied by each mode exactly due to ansatz (3.14), when the original two-dimensional

https://doi.org/10.1017/jfm.2013.584 Published online by Cambridge University Press

boundary value problem is reduced to one-dimensional eigenvalue problems (4.1) or (3.20) depending on whether the current is assumed weak in intensity or slowly varying in the transverse direction. The problem (3.20) may be reformulated in the form of eigenvalue problem (4.6) with dispersion relation (4.11).

To validate the developed asymptotic approach and to estimate its accuracy, the original boundary value problem in the (y, z) plane is solved numerically without invoking the separation of variables. The approach follows the methodology presented in § 3.2: the modes are sought in the form of combinations of functions $Y(y)Z(z)$ constrained by the compatibility condition (3.7); the details are given in appendix E. The two-dimensional problem is solved using a perturbation technique which is valid when the combination of parameters $\rho \equiv \gamma\mu^2$ satisfies $\rho < 1$. At the lowest order (3.2) is reduced to the Helmholtz equation; then the boundary value problem admits a numerically exact solution.

In this section we treat these numerical solutions of the original two-dimensional boundary value problem as 'exact' and compare them with the leading-order asymptotic solutions provided by the one-dimensional eigenvalue problems: the Sturm–Liouville one for weak currents (4.6) and the nonlinear one for broad currents (4.1). The solutions resulting from these different approaches are distinguished by the subscripts denoting the relevant small parameters, i.e. as $\hat{w}_\rho$, $\hat{w}_\gamma$ and $\hat{w}_\mu$ respectively. The solutions we examine here are for the same example of a sech-squared current.

The Sturm–Liouville problem (4.6) for weak sech-squared currents yields the solution in the form of Legendre functions (see § C.2). The nth mode vertical velocity in the entire domain of the fluid is given by $\hat{w}_\gamma = Y_n(y)Z_n(y, z)$, where Y_n is the nth transverse mode of (C 7) with the corresponding vertical structure $Z_n = \exp(\Omega_n^2(y)/gz)$, where ω_n is found according to (4.11).

The second asymptotic solution we examine employs the broad current expansion, which allows the current to be strong; the corresponding eigenvalue problem is given by (4.1). It involves the eigenvalue (frequency or wavenumber) in a nonlinear fashion, and thus is difficult for analytic analysis, though (4.1) may be easily solved numerically. To this end the second-order equation (4.1) is written in the form of a couple of first-order differential equations; then the eigenvalue problem for ω_n is solved using the shooting method. The integration in y is performed by means of the fourth-order Runge–Kutta method. Recall that eigenfrequencies ω_n and the dispersion relations for trapped modes were obtained in § 4.5 and shown in figure 2(*d*) by circles. Modal functions $Y_n(y)$ are obtained in this way as well. Similar to the analytic solution of the Sturm–Liouville problem, the two-dimensional mode is then constructed as $\hat{w}_\mu(y, z) = Y_n(y)Z_n(y, z)$, where $Z_n = \exp(\Omega_n^2(y)/gz)$.

A deliberately unrealistic extremely strong and narrow sech-squared current is chosen for testing the two asymptotic solutions formulated above, $U_0 = -5$ m s^{-1}, $L = 200$ m – the same parameters as used in figure 2(*d*), and discussed in appendix E. We consider two values of the longitudinal wavenumbers, $k = 0.1$ rad m^{-1} and $k = 0.06$ rad m^{-1}, corresponding to $\gamma = 0.5, 0.4$ and $\mu = 0.05, 0.08$. For the shorter waves the Sturm–Liouville problem (4.6) predicts 28 trapped modes in total; only 15 trapped modes exist in the longer wave case. The solution of the boundary value problem (4.1) yields 34 and 18 trapped modes respectively. The numerical reference solution of the original two-dimensional problem (3.2) and (3.7) returns 35 and 19 modes.

All the solutions, $\hat{w}_\rho$, $\hat{w}_\gamma$, $\hat{w}_\mu$, look qualitatively similar. The profiles of the 15th ($n = 14$) trapped mode on the surface, $z = 0$, are shown in figure 3(*a*). Figure 3(*b*) illustrates the comparison between the modes in the plane (y, z); here the upper

https://doi.org/10.1017/jfm.2013.584 Published online by Cambridge University Press

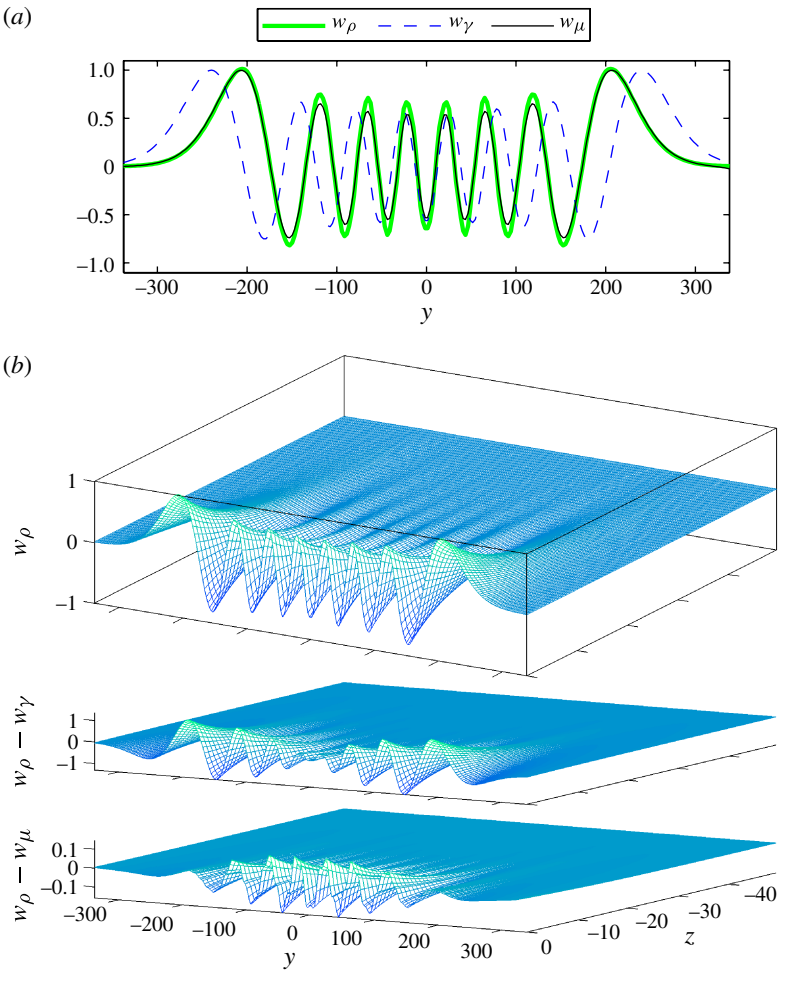


FIGURE 3. (Colour online) The reference solution of the original two-dimensional boundary value problem ($\hat{w}_\rho$), solutions of the approximate Sturm–Liouville problem for weak currents (4.6) ($\hat{w}_\gamma$), and of the problem for broad currents (4.1) ($\hat{w}_\mu$), for the sech-squared current with $U_0 = -5$ m s^{-1} and $L = 200$ m (the same characteristics as in figure 2*d*, $k = 0.1$ rad m^{-1}), $n = 14$. (*a*) Modes on the free surface, $z = 0$; (*b*) top, $\hat{w}_\rho(y, z)$; below, $\hat{w}_\rho - \hat{w}_\gamma$ and $\hat{w}_\rho - \hat{w}_\mu$ correspondingly.

surface is the numerical reference solution of the original two-dimensional boundary value problem, $\hat{w}_\rho$. The plots below present the discrepancies between the solutions of the weak-current Sturm–Liouville and the broad-current nonlinear boundary value problems and the reference solution, respectively.

The figure demonstrates that the modal structure is very similar in all the solutions, although the precise locations of the maxima at the periphery of the jet are not captured perfectly, which gives the main contribution to the discrepancy. The maximal values of the discrepancies between $\hat{w}_\rho$ and $\hat{w}_\gamma$, and $\hat{w}_\rho$ and $\hat{w}_\mu$ may be seen in figure 3(*b*), and in table 1. Table 1 also provides additional insight by presenting the maxima and root mean square of the similar discrepancies for a few modes and for

https://doi.org/10.1017/jfm.2013.584 Published online by Cambridge University Press

Longitudinal wavenumber, k (rad m^{-1})	Mode, $n+1$	Maximum difference in $\hat{w}$ weak/broad current (%)	r.m.s. discrepancy in $\hat{w}$, weak/broad current (%)	Difference in ω, weak/broad current (%)
0.06	1	1.3/1.5	1.5/2.1	0.09/0.2
0.06	5	30/8.9	25/6.0	−1.9/0.06
0.06	15	148/14	156/7.7	−1.2/−0.008
0.1	1	0.8/1.1	0.9/1.2	0.06/0.1
0.1	5	22/6.4	18/4.7	−1.5/0.07
0.1	15	137/16	123/10	−5.1/0.01

TABLE 1. Accuracy of the asymptotic solutions. The numerical solution of the original two-dimensional boundary value problem, $\hat{w}_\rho(y,z)$, is taken as the reference. Three columns list the relative maximum discrepancy, the r.m.s. discrepancy and the relative difference in eigenfrequency for the solutions in the weak/broad current approximations.

two longitudinal wavenumbers; the discrepancy becomes of order one when the mode number, n, approaches its maximal value. Figure 3(b) shows that the maxima of the discrepancies are located near or on the water surface. The example in figure 3(a) shows that the large $\max|\hat{w}_\rho - \hat{w}_\gamma|$ is mainly due to significant lateral stretching of the mode. It may be concluded from table 1 and figure 3 that the broad-current approximation results in much better description of the modes, except the lowest mode. It also generally provides more accurate eigenfrequencies, though the solution of the Sturm–Liouville problem gives rather accurate estimates as well. We stress that the comparison in figure 3 was presented for the high-number 15th mode, i.e. for one of the least favourable situations.

Thus, the asymptotic solutions represented by the leading-order one-dimensional boundary value problems (4.1) and (4.6) are shown to be capable of faithfully describing solutions to the original two-dimensional problem, even when the current is extremely strong and narrow in the transverse direction. We emphasize that the chosen current speed, 5 m s^{-1}, is comparable to the wave phase velocities, $\sqrt{g/k} \sim 10 \ldots 13$ m s^{-1}, for the chosen wavenumbers. The characteristic wavelengths, $2\pi/k$, are of order 10^2 m, while the characteristic half-width of the current is unrealistically narrow: 200 m. Even for such an extreme case the low modes are captured very accurately by both expansions.

The description based upon a tractable one-dimensional boundary value problem may be further improved when a higher-order theory is employed (see appendix B). Estimates and discussion of the accuracy of the Sturm–Liouville problem as the limit of the broad-current approximation are given in appendix D.

6. Discussion

6.1. *The key points of the approach*

First we briefly summarize our approach to the description of waves on jet currents. The present paper is confined to linear wave dynamics, and its main aim is to prepare the ground for systematic examination of nonlinear dynamics in subsequent parts of the work. It makes sense to begin with explicit and implicit assumptions. The most crucial assumption is the neglect of the vertical shear of currents. At present we can only say that in the majority of situations of wave–current interaction observed in nature, as we will illustrate with a few examples below, the vertical

https://doi.org/10.1017/jfm.2013.584 Published online by Cambridge University Press

shear is small. This smallness in itself does not justify *a priori* neglect of the vertical shear: qualitatively new effects caused by shear cannot be ruled out. The issue requires a dedicated study which goes beyond the scope of the present work. The deep water approximation is adopted for simplicity only: it is straightforward to extend the approach to finite depth situations where waves are affected by both the current and the bottom topography. This will result in a somewhat different boundary value problem describing a broad range of situations: we will recover the present results in one limit and edge type waves in another. A proper analysis of the rich variety of possible regimes requires special consideration. To introduce the concept of modal description in the simplest possible way we also assumed homogeneity of the current with respect to the longitudinal coordinate. The effects due to mild longitudinal inhomogeneity are numerous and important; we will discuss the issue in a dedicated paper.

Under the above assumptions we have shown that an asymptotic separation of variables which underpins the modal description of the wave field on currents is possible if either of the two natural parameters $\mu = (kL)^{-1}$ and $\gamma = |U_{max}/C|$ is small: see the scheme in figure 1. The reason is that the employed asymptotic separation of variables exploits asymptotically slow transverse dependence of the vertical decay exponent; this slowness is estimated to be $O(\gamma\mu)$. The developed asymptotic scheme enables us to obtain a solution as an asymptotic series to any desired accuracy, although the higher-order terms in the expansion are quite cumbersome.

For strong broad currents with $\gamma \sim 1$, the boundary value problem specifying the dispersion relation and the transverse modes has a non-standard form: the eigenmodes are not orthogonal, although it is straightforward for numerical integration. For each longitudinal wavenumber and the trapped mode number the boundary value problem uniquely determines the wave frequency and the mode shape. Even the strongest currents in the ocean are, as a rule, weak in the sense that $\gamma \ll 1$. For such situations the boundary value problem reduces to the classical Sturm–Liouville type based upon the stationary Schrödinger equation, and the current broadness is not required. Thus the modes (trapped and passing-through) form a complete orthogonal set. This makes the modal description of waves on currents a mathematically attractive alternative to currently adopted approaches, at least in situations where there are no critical layers.

The currently prevailing WKB approach requires the transverse scale of the current variation, L, to be large compared to the lateral scale of the wave field variation $k^{-1}\chi^{-1}$. Hence for the WKB applicability the somewhat restrictive condition $\mu/\chi \ll 1$ should hold. It is also worth mentioning that the classical WKB approach does not describe the wave field at the caustics, i.e. near the turning points and, crucially, since the low modes have transverse scales comparable to the width of the current, cannot describe the low modes in which we are particularly interested. From the mathematical viewpoint the inapplicability of the WKB approach for the low modes stems from the close proximity of the two turning points: they cannot be treated as isolated.

The asymptotic approach developed here for surface waves can be extended to internal gravity waves on currents. However, some modifications are needed. This goes beyond the scope of the present work and will require a dedicated study.

6.2. *Ocean currents through the prism of trapped waves*

The idea that all ocean currents can support trapped waves has been around for at least four decades. The theoretical basis underpinning the idea was the WKB or ray theory for linear waves (e.g. Kenyon 1971; Peregrine 1976). The observations confirming the existence of trapped waves are more recent (Kudryavtsev *et al.* 1995). Our asymptotic

https://doi.org/10.1017/jfm.2013.584 Published online by Cambridge University Press

approach does not require the WKB approximation and relies on the existence of two independent small parameters γ and μ. The key point we want to reiterate before discussing specific ocean currents is that for dominant waves of scales $\sim 10^2$ m with characteristic celerities $\sim 10^1$ m s^{-1}, all oceanic currents are weak, hence $\gamma \ll 1$; most of the currents are also broad. Of course, there are also contexts in which waves of scales smaller compared to the dominant ones are of primary interest.

The Agulhas Current off the east coast of southern Africa is probably the most infamous place in terms of the number of documented rogue-wave-on-current accidents, see e.g. Mallory (1974). On the other hand, the Agulhas Current is a fairly typical representative of western boundary currents in the ocean and it is worthwhile discussing the current through the prism of the theory presented in the paper. Hopefully such a consideration being of interest for its own sake will also help us one day to understand why the Agulhas Current is so special, or under what conditions we can expect rogue wave event for a particular current.

The Agulhas Current follows the continental shelf southward from Maputo to the tip of the Agulhas Bank (Cape Agulhas). A comprehensive description of this current can be found in Lutjeharms (2006). In our context the most relevant characteristics are the bottom topography and the typical distribution of the current velocity in the cross-section of the current. These characteristics for a particular cross-section chosen to be off Durban at the latitude 30° S are shown in figure 4(*a*). The interpolated data from Toole & Raymer (1985) have been used. We note that the vertical shear is indeed relatively weak, $U_z \sim 10^{-3}$ s^{-1}, which *a posteriori* to some extent justifies its total neglect in our consideration, at least as a reasonable first approximation. The shelf slope is quite steep between Durban and East London, and the main core of the current is confined to the seaward side of the continental shelf. For the scales under consideration the deep water approximation seems to be totally adequate.

The current exhibits substantial seasonal and inter-annual variations. According to Mallory (1974), its maximum speed may attain 2–2.5 m s^{-1}, while the width varies from 90 to 160 km. Lutjeharms (2006) gives an estimate of monthly mean velocity in the core of the current of $\sim$1.6 m s^{-1}, while the peak speed is $\sim$2.8 m s^{-1}. The current profile in figure 4(*a*) is taken from Toole & Raymer (1985), who report the maximum magnitude of $\sim$1.2 m s^{-1}. For the surface wave dynamics the most relevant is the surface layer. The horizontal cross-section of the current figure 4(*a*) at the depth 20 m is given in figure 4(*c*) by circles, and then extrapolated employing a cubic spline (the curve in figure 4*c*). Note that Lavrenov (1998) used another characteristic shape of the current with the maximum velocity $\sim$2 m s^{-1}.

One of the peculiar features of the Agulhas Current is its strong intermittent narrow counter-current located closer to the shore, as shown in figure 4(*b*). Its typical maximal speed is about half of the peak velocity in the main stream or less and the width is 10–20 km or even less. We will not pursue this counter-current any further, merely note its existence. For simplicity we will base most of our estimates on the Toole & Raymer (1985) approximation of the current profile shown in figure 4(*c*).

First we estimate the number of trapped modes using the approximate Bohr–Sommerfeld formula (4.8). The integral in (4.8) is evaluated numerically for the profile shown in figure 4(*a,c*), and the number of trapped modes, N_{tr}, is plotted in figure 5 as function of the wavelength. For typical wind waves of wavelengths $\sim 10^2$ m and swell of lengths 3–5 $\times$ 10^2 m, the phase velocities are $\sim 10^1$ m s^{-1}, so the Agulhas Current can support a large number of trapped modes: $\sim 10^3$ for wind waves and $\sim 2 \times 10^2$ for swell. The number of modes trapped by a typical counter-current is 40 and 5 for wind waves and swell respectively. For the estimates the counter-current

https://doi.org/10.1017/jfm.2013.584 Published online by Cambridge University Press

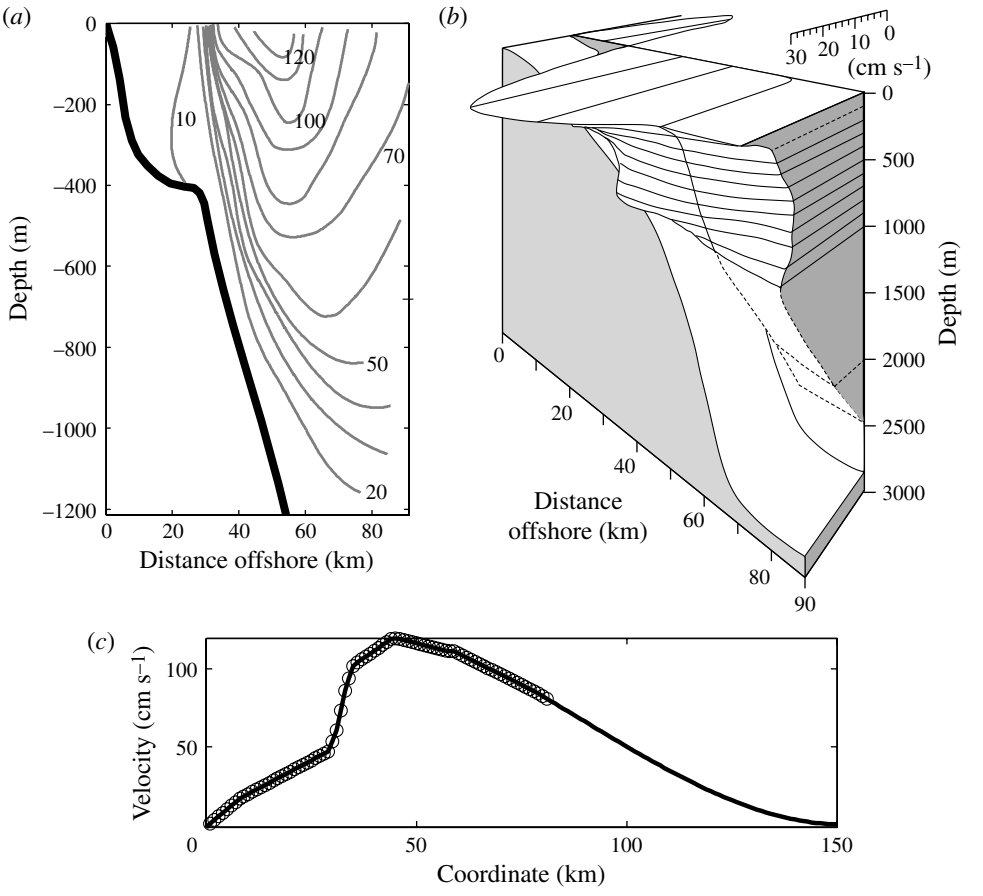


FIGURE 4. Zonal cross-section of the Agulhas Current. (*a*) Typical velocity distribution at the latitude 30° S according to Toole & Raymer (1985). Isolines show velocities in cm s^{-1}. The thick line is the bottom. (*b*) Vertical and horizontal structure of the Agulhas Current downstream of Durban, with evidence of the counter-current (Lutjeharms 2006). (*c*) The transverse horizontal velocity distribution at the depth 20 m. Circles show the data from (*a*), and the curve is the result of cubic spline extrapolation.

was assumed to have magnitude 0.5 m s^{-1} and width 5 km. While the waves trapped by the main current propagate towards the equator, obviously the waves trapped by the counter-current propagate towards the pole.

It is also of interest to estimate the Doppler correction to the trapped wave frequency due to an opposing current. We estimate the relative Doppler shift as $kU_{max}/\sqrt{kg} \sim U_{max}/C$, where C is the characteristic wave phase velocity. For example, a long 17 s swell with corresponding length ∼450 m and phase speed 27 m s^{-1} yields $kU_{max}/\sqrt{kg} \approx 0.05$. Recall that the number of trapped modes for this wavelength is estimated as 200 (see figure 5), and hence the relative difference between the neighbouring frequencies corresponding to different modes can be estimated as $|\omega_{n+1} - \omega_n|/\omega_n \sim 2 \times 10^{-4}$. When the sech-squared shape is fitted to model the Aghulas Current, and exact solution (C 9) for the sech-squared current is used to plot a figure similar to figure 2(*b*), the lines representing different trapped modes are too dense to be distinguished with the naked eye.

https://doi.org/10.1017/jfm.2013.584 Published online by Cambridge University Press

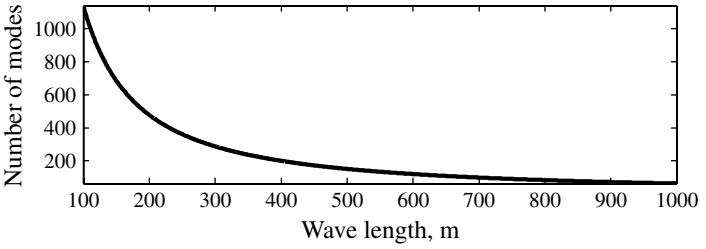


FIGURE 5. The number of trapped modes supported by the Agulhas Current as a function of wavelength.

We are unaware of any *in situ* observations of trapped waves on the Agulhas Current, although there are satellite SAR observations of waves on the Agulhas Current which admit such interpretation but are not supported by any concomitant direct measurements (e.g. Irvine & Tilley 1988). Well-pronounced trapped waves with significant wave height roughly twice to three times the value outside the jet and significant whitecap coverage in spite of a wind speed decrease were observed on the Gulf Stream by Kudryavtsev *et al.* (1995) under conditions less favourable for trapped modes than those typical of the Agulhas Current. In Kudryavtsev *et al.* (1995) these trapped wave systems were also modelled using the kinetic equation with refraction terms and the nonlinear term taken in the crude but easy-to-handle relaxation approximation: fairly good agreement with the observations was found. Within the linear ray theory framework Kenyon (1971) estimated the minimum angle between the wave vector and the current normal at the position of maximum current speed for the conditions of the Gulf Stream. It proved to be surprisingly large; similar estimates are equally valid for the Agulhas Current. Taking the maximum current speed to be 2 m s^{-1}, Kenyon (1971) found that the minimum angle is greater than 48° for 8 s waves and exceeds 59° for 16 s waves. In our consideration, we estimate the minimum angle following Kenyon (1971) to be

$$\alpha_{min} = \arctan \frac{k}{\max k_y} \quad \text{where } k_y = \sqrt{-l^2 - k^2 \frac{4kU_m}{\sqrt{kg}}}; \tag{6.1}$$

on setting $k \approx \omega^2/g$ and $l = 0$, the resulting estimate yields angles 51 and 60° for 8 s and 16 s waves respectively.

Our discussion of oceanic western boundary currents as exemplified by the Agulhas Current can be summarized as follows: (i) such currents support a large number (10^2–10^3) of trapped modes; (ii) these modes are not just handy mathematical constructs but have been observed *in situ*; (iii) compared to other western boundary currents the Agulhas looks fairly typical, and the role of its only special feature, the counter-current, is not clear. At present we only hypothesize the existence of unstable trapped modes amplified through the critical layer mechanism by the counter-current; this hypothesis needs dedicated study to be elaborated.

Another important class of the oceanic currents is that of zonal currents, such as the Antarctic Circumpolar Current (ACC), the largest current in the ocean. We are unaware of any observations of trapped modes on zonal currents. Such currents are usually much wider than western boundary currents. Correspondingly, the natural requirement for the time scale needed for formation of trapped modes to be smaller than the nonlinear interaction time scale becomes quite restrictive. We can

https://doi.org/10.1017/jfm.2013.584 Published online by Cambridge University Press

roughly estimate the trapped mode formation time scale as $\sim L/C^0_{g(y)}$, where L is the characteristic width of the current and $C^0_{g(y)}$ is the transverse component of the characteristic group wave velocity in the WKB approximation taken in the maximum of the current. For example, the characteristic width of the ACC is $\approx 10^3$ km, if we take 'average' $C_{g(y)}$ to be $O(1)$ m s^{-1}; then the characteristic time of mode formation is 10^6 s, i.e. $\sim 10^1$ days. Certainly such a time scale far exceeds the time scale of wave nonlinear interactions $\omega^{-1}\varepsilon^{-4}$, which makes formation of the current-wide trapped modes of wind waves practically impossible. On the other hand, it is worth noting that broad zonal currents are often made up of several streams which could be much narrower, as is the case for the ACC (e.g. Orsi, Whitworth & Nowlin 1995; Rintoul, Hughes & Olbers 2001).

The conditions are more favourable for smaller-scale currents such as tidal currents in relatively shallow waters, rip and longshore currents (e.g. Galvin 1967; Thornton & Guza 1986; Dalrymple *et al.* 2011). It should be noted that for all these situations the deep water approximation is often not applicable at all. For longshore and tidal currents the topography might be equally as important or even more important in creating waveguides, which leads to the necessity of considering a boundary value problem with transverse inhomogeneity provided by both the current and bottom topography. For rip currents and longshore currents their speed is small compared to typical wind waves and swell, i.e. all such currents automatically fall into the class with $\gamma \ll 1$, while the broadness parameter μ could be as big as order one.

We conclude by reiterating that in this paper we confine our attention to the currents which can be reasonably approximated by plane parallel jets, and do not discuss currents of different geometry, which requires special consideration. Here we just mention that the currents with axial symmetry, such as idealized models of vortices and rings, also allow separation of variables; however, an asymptotic procedure reducing the resulting boundary value problem to solving a one-dimensional problem has yet to be developed. The findings of this work for the given plane geometry provide the foundation for a systematic mathematical description of nonlinear dynamics of waves on jets, which will be discussed in the follow-up papers.

Acknowledgements

The authors are thankful to C. J. Chapman for helpful discussions and comments on the first draft of the paper. The authors gratefully acknowledge support from the European Commission Seventh Framework Programme (grant PIIF-GA-2009-254389) without which the work might never have happened. A.S. is grateful to colleagues in the Department of Mathematics and EPSAM at Keele for warm hospitality. A.S. also acknowledges partial support from RFBR grants 11-02-00483 and 12-05-33087.

Appendix A. Ansatz for the vertical mode structure

In this section we outline our reasoning behind the chosen form of ansatz (3.14). Recall that according to (3.11), the vertical mode $Z_n(z, y)$ for the deep water case is an exponential function to the leading order. To find a convenient general ansatz for this function, we proceed as follows. We replace the surface boundary condition (3.7) by the following condition in the vicinity of the free surface:

$$\frac{\partial \hat{w}}{\partial z} = \frac{\Omega^2}{g}\hat{w} + q(z, y)\hat{w} \quad \text{as } z \to 0, \tag{A 1}$$

https://doi.org/10.1017/jfm.2013.584 Published online by Cambridge University Press

where $q(z, y)$ is a smooth function for all allowed y and z satisfying $q(0, y) = 0$; we will specify $q(z, y)$ below. It reduces to (3.7) when $z = 0$. We assume that each nth mode obeys the boundary condition, and then for each n taking into account (3.13), condition (A 1) yields

$$\frac{\partial Z_n}{\partial z} = h_n(y) Z_n + q(z, y) Z_n \quad \text{at } z = 0 \tag{A 2}$$

for all n. This condition may be integrated once, which results in

$$Z_n(z, y) = \Gamma_n(z, y) \exp(h_n(y) z) \quad \text{where } \Gamma_n = Z_n(z_0, y) \exp\left(\int_{z_0}^{z} q(\xi, y)\, \mathrm{d}\xi \right). \tag{A 3}$$

Note that since $q(0, y) = 0$, then $(\partial \Gamma_n / \partial z)|_{z=0} = 0$. It is evident that a smooth function $\Gamma_n(z, y)$ may then be represented in the form $\Gamma_n = \alpha_n(y)[1 + z^2 f_n(z, y)]$, where $\alpha_n(y)$ and $f_n(y)$ are some new functions. The unspecified function $\alpha_n(y)$ may be incorporated into the modal function $Y_n(y)$ in (3.13), and hence may be set equal to one. Hence we arrive at the expression for $Z_n(z, y)$ in the form (3.14).

Appendix B. Asymptotic reduction of the original two-dimensional boundary value problem to the one-dimensional problem on transverse modes

Consideration of the system of equations (3.2) and (3.7) at different orders of a small parameter enables one to solve the problem asymptotically. Condition (3.7) specifies h_n as a function of k and ω_n. The problem (3.2) links k and ω_n and specifies lateral modes. Details of the asymptotic theory briefly outlined in § 3.3 are presented below to second order in the natural small parameters γ and μ.

First recall the basic points of the procedure. We assume that the problem allows approximate separation of variables, so that the vertical component of fluid velocity may be represented in the form

$$\hat{w} = \sum_n B_n Y_n(y) Z_n(z, y), \tag{B 1}$$

where $Z_n(z, y)$ is a slow function of y, so that function $Y_n(y)$ is the major part of the transverse variation of $\hat{w}$, and to leading order the vertical mode has an exponential dependence, $Z_n(z, y) \sim \exp(h_n(y) z)$. The eigenfrequency ω_n, separation function h_n, and $\hat{w}$ are then sought in the form of an asymptotic series in the small parameter reflecting the slowness of the lateral dependence of Z_n. There are two possibilities for choosing the small parameter in the asymptotic expansion.

B.1. *Weak currents*

First consider weak currents and employ the smallness of γ, while assuming μ to be of order one. For convenience we introduce another small parameter, $\chi \sim \sqrt{\gamma}$, which is a characteristic non-dimensional transverse wavenumber: see (3.17). The asymptotic series are specified by (3.15) and (3.16), as follows:

$$\omega_n = \omega_n^{(0)} + \chi^2 \omega_n^{(1)} + \chi^4 \omega_n^{(2)} + \cdots, \tag{B 2a}$$

$$h_n(y) = h_n^{(0)} + \chi^2 h_n^{(1)} + \chi^4 h_n^{(2)} + \cdots, \tag{B 2b}$$

$$\hat{w}_n(y, y_\chi, z) = \hat{w}_n^{(0)} + \chi \hat{w}_n^{(1)} + \chi^2 \hat{w}_n^{(2)} + \chi^3 \hat{w}_n^{(3)} + \chi^4 \hat{w}_n^{(4)} + \cdots, \tag{B 2c}$$

https://doi.org/10.1017/jfm.2013.584 Published online by Cambridge University Press

and

$$\hat{w}_n^{(0)}(y, y_\chi, z) = B_n^{(0)} Y_n^{(0)} \overline{Z}_n, \tag{B 3a}$$

$$\hat{w}_n^{(1)}(y, y_\chi, z) = B_n^{(1)} Y_n^{(1)} \overline{Z}_n, \tag{B 3b}$$

$$\hat{w}_n^{(2)}(y, y_\chi, z) = B_n^{(2)} (Y_n^{(2)} + z^2 Y_n^{(22)}) \overline{Z}_n, \tag{B 3c}$$

$$\hat{w}_n^{(3)}(y, y_\chi, z) = B_n^{(3)} (Y_n^{(3)} + z^2 Y_n^{(32)}) \overline{Z}_n, \tag{B 3d}$$

$$\hat{w}_n^{(4)}(y, y_\chi, z) = B_n^{(4)} (Y_n^{(4)} + z^2 Y_n^{(42)} + z^3 Y_n^{(43)} + z^4 Y_n^{(44)}) \overline{Z}_n, \tag{B 3e}$$

$$\overline{Z}_n(y, z) = \exp(h_n z). \tag{B 3f}$$

We also introduce a slow transverse coordinate, $y_\chi \equiv \chi y$, assuming that all functions which describe the lateral mode structure are functions of the slow coordinate, $Y_n^{(\dots)}(y_\chi)$. All other functions depend on the fast coordinate, y, including $h_n^{(\dots)}(y)$; the smallness of the derivative with respect to y is due to the smallness of y-dependent components h_n. Note that in the next subsection, which deals with μ expansions, h_n will depend on the slow coordinate. Constants $B_n^{(\dots)}$ are to be determined.

The differentiation operator in the lateral direction then operates as follows, $\partial_y \to \partial_y + \chi \partial_{y_\chi}$.

To leading order $O(\chi^0)$, the waves are ordinary surface deep water waves, and the problem, specified by (3.7) and (3.2), gives the classical dispersion relation,

$$h^{(0)} = k, \quad \omega^{(0)2} = gk. \tag{B 4}$$

To order $O(\chi^1)$ no new terms appear in the dispersion relation. To order $O(\chi^2)$ we arrive at the leading-order boundary value problem

$$h^{(1)}(y) = 2k \frac{\Omega^{(1)}}{\omega^{(0)}} \quad \text{where } \Omega^{(1)} \equiv \omega^{(1)} - kU(y), \tag{B 5}$$

and

$$z \left[4kY^{(22)} - 2\frac{k^2}{\omega^{(0)}} Y^{(0)} \frac{\partial^2 U}{\partial y^2} \right] + z^0 \left[\frac{\partial^2 Y^{(0)}}{\partial y_\chi^2} + \frac{4k^2}{\omega^{(0)}} \Omega^{(1)} \right] = 0. \tag{B 6}$$

Expressions in brackets at different powers of z in (B 6) do not depend on the vertical coordinate, and hence each of them must be equal to zero. The terms in the first brackets specify auxiliary function $Y^{(22)}$, and terms in the second brackets constitute the boundary value problem on the first-order frequency correction $\omega^{(1)}$, which may be written in the form

$$\widehat{L}_\gamma Y^{(0)} = 0 \quad \text{where } \widehat{L}_\gamma Y \equiv \frac{\partial^2 Y}{\partial y_\chi^2} - \left[4\frac{k^3 U}{\sqrt{kg}} - 4k^2 \frac{\omega^{(1)}}{\omega^{(0)}} \right] Y. \tag{B 7}$$

To order $O(\chi^3)$, relation (3.7) is satisfied, and (3.2) results in

$$z \left[4kY^{(32)} - 2\frac{k^2}{\omega^{(0)}} Y^{(1)} \frac{\partial^2 U}{\partial y^2} - 4\frac{k^2}{\omega^{(0)}} \frac{\partial U}{\partial y} \frac{\partial Y^{(0)}}{\partial y_\chi} \right] + z^0 \left[\widehat{L}_\gamma Y^{(1)} + G_1 \right] = 0$$

$$\text{where } G_1 = \frac{2k}{\omega^{(0)}} \frac{\partial U}{\partial y} \frac{\partial Y^{(0)}}{\partial y_\chi}. \tag{B 8}$$

Similar to the above, the terms in the first brackets specify function $Y^{(32)}$, while the terms in the second brackets constitute the inhomogeneous differential equation which

https://doi.org/10.1017/jfm.2013.584 Published online by Cambridge University Press

specifies function $Y^{(1)}$,

$$\widehat{L}_\gamma Y^{(1)} + G_1 = 0. \tag{B 9}$$

The next order, $O(\chi^4)$, adjusts function h,

$$h^{(2)} = 2k\frac{\omega^{(2)}}{\omega^{(0)}} + k\frac{\Omega^{(1)2}}{\omega^{(0)2}}. \tag{B 10}$$

Then relation (3.2) gives

$$\begin{aligned}
&z^3\left[8kY^{(44)} - \frac{k^3}{\omega^{(0)2}}\left(\frac{\partial^2 U}{\partial y^2}\right)^2 Y^{(0)}\right] \\
&+ z^2\left[6kY^{(43)} + 12Y^{(44)} - \frac{k^2}{2\omega^{(0)2}}\left(\frac{\partial^2 U}{\partial y^2}\right)^2 Y^{(0)} + 4\frac{k^4}{\omega^{(0)2}}\left(\frac{\partial U}{\partial y}\right)^2 Y^{(0)}\right] \\
&+ z\left[4kY^{(42)} + 6Y^{(43)} - 2\frac{k^2}{\omega^{(0)}}\frac{\partial^2 U}{\partial y^2}Y^{(2)} - 4\frac{k^2}{\omega^{(0)}}\frac{\partial U}{\partial y}\frac{\partial Y^{(1)}}{\partial y_\chi}\right. \\
&\left. + 2\frac{k^2\omega^{(1)}}{\omega^{(0)2}}\frac{\partial^2 U}{\partial y^2}Y^{(0)} - 2\frac{k^3}{\omega^{(0)2}}U\frac{\partial^2 U}{\partial y^2}Y^{(0)} + 2\frac{k^3}{\omega^{(0)2}}\left(\frac{\partial U}{\partial y}\right)^2 Y^{(0)}\right] \\
&+ z^0\left[\widehat{L}_\gamma Y^{(2)} + G_2\right] = 0, \\
&\text{where } G_2 = 4\omega^{(2)}\frac{k^2}{\omega^{(0)}}Y^{(0)} + \frac{2k}{\omega^{(0)}}\frac{\partial U}{\partial y}\frac{\partial Y^{(1)}}{\partial y_\chi} \\
&+ \frac{1}{2\omega^{(0)2}}\left(\frac{\partial^2 U}{\partial y^2}\right)^2 Y^{(0)} + 6\frac{k^2\Omega^{(1)2}}{\omega^{(0)2}}Y^{(0)} - \frac{k^2}{\omega^{(0)2}}\left(\frac{\partial U}{\partial y}\right)^2 Y^{(0)}.
\end{aligned} \tag{B 11}$$

The terms in brackets at different powers of z must be equal to zero; this requirement specifies line-by-line functions $Y^{(44)}$, $Y^{(43)}$ and $Y^{(42)}$ respectively. Explicit forms of these auxiliary functions are used to simplify the expression for G_2. Terms at z^0 constitute the inhomogeneous problem for determining second-order corrections to the mode function $Y^{(2)}$ and to the frequency, $\omega^{(2)}$,

$$\widehat{L}_\gamma Y^{(2)} + G_2 = 0. \tag{B 12}$$

After multiplication of (B 12) by $Y^{(0)}$, integration over y and making use of (B 7) and (B 9), frequency correction $\omega^{(2)}$ is obtained. Then, (B 12) is an inhomogeneous ordinary differential equation specifying $Y^{(2)}$. Higher-order asymptotic terms may be obtained in a similar fashion, although the derivation becomes rather tedious.

B.2. *Broad currents*

In the case of a broad current, that is, $U = U(\mu y)$, series in powers of $\mu \ll 1$ are employed (see (3.22) and (3.23)), while γ is assumed to be of order one. The subsequent limit when γ is small is considered in § 4.2.

The asymptotic scheme outlined in § 3.3.2 and given in more detail below exploits the fact that the smoothness of the current, $U(y_\mu)$, where $y_\mu \equiv \mu y$ is a new slow transverse coordinate, implies that $h_n = h_n(y_\mu)$, that is, h_n is a slow function of y.

https://doi.org/10.1017/jfm.2013.584 Published online by Cambridge University Press

The asymptotic series have a somewhat different form in comparison to the previous case of weak currents:

$$\omega_n = \omega_n^{(0)} + \mu\omega_n^{(1)} + \mu^2\omega_n^{(2)} + \cdots, \tag{B 13a}$$

$$h_n(y_\mu) = h_n^{(0)} + \mu h_n^{(1)} + \mu^2 h_n^{(2)} + \cdots, \tag{B 13b}$$

$$\hat{w}_n(y, y_\mu, z) = \hat{w}_n^{(0)} + \mu\hat{w}_n^{(1)} + \mu^2\hat{w}_n^{(2)} + \cdots, \tag{B 13c}$$

and

$$\hat{w}_n^{(0)}(y, y_\mu, z) = B_n^{(0)} Y_n^{(0)} \overline{Z}_n, \tag{B 14a}$$

$$\hat{w}_n^{(1)}(y, y_\mu, z) = B_n^{(1)} (Y_n^{(1)} + z^2 Y_n^{(12)}) \overline{Z}_n, \tag{B 14b}$$

$$\hat{w}_n^{(2)}(y, y_\mu, z) = B_n^{(2)} (Y_n^{(2)} + z^2 Y_n^{(22)} + z^3 Y_n^{(23)} + z^4 Y_n^{(24)}) \overline{Z}_n, \tag{B 14c}$$

$$\overline{Z}_n(y_\mu, z) = \exp(h_n z). \tag{B 14d}$$

Functions $Y_n^{(\ldots)}$ depend on the fast coordinate, and y and $B_n^{(\ldots)}$ are constants.

To leading order $O(\mu^0)$, the approach results in the relation between the eigenfrequency and wavenumber and the separation function

$$g h^{(0)}(y_\mu) = \Omega^{(0)2} \quad \text{where } \Omega^{(0)} \equiv \omega^{(0)} - kU(y_\mu), \tag{B 15}$$

and the boundary value problem

$$\widehat{L}_\mu Y^{(0)} = 0 \quad \text{where } \widehat{L}_\mu Y \equiv \frac{\partial^2 Y}{\partial y^2} + [h^{(0)2} - k^2] Y. \tag{B 16}$$

To $O(\mu^1)$, relation (3.7) requires

$$h^{(1)} = 2\frac{\omega^{(1)}}{g}\Omega^{(0)}, \tag{B 17}$$

and (3.2) gives

$$z^2 \widehat{L}_\mu Y^{(12)} + z\left[4h^{(0)} Y^{(12)} + 2\frac{\partial Y^{(0)}}{\partial y}\frac{\partial h^{(0)}}{\partial y_\mu}\right] + z^0\left[\widehat{L}_\mu Y^{(1)} + F_1\right] = 0,$$

$$\text{where } F_1 = 2Y^{(12)} + 4\omega^{(1)}\frac{\Omega^{(0)3}}{g^2} Y^{(0)}. \tag{B 18}$$

The terms at different powers of z do not depend on the vertical coordinate, so each of them must be equal to zero. Since function $h^{(0)}$ is never equal to zero, the requirement of the content of the first brackets in (B 18) to be zero determines function $Y^{(12)}$; hence, $Y^{(12)}$ is expressed in terms of $Y^{(0)}$ and $h^{(0)}$. Given that $h^{(0)}$ is a slow function of y, the first term in (B 18) is smaller than $O(\mu)$ by virtue of the definition of the operator $\widehat{L}_\mu$ (B 16), and therefore falls out to the next asymptotic order. The remaining terms in (B 18) at z^0 constitute the inhomogeneous problem specifying $Y^{(1)}$ and $\omega^{(1)}$, similar to § B.1.

The derivation of higher-order asymptotic solutions, although straightforward in principle, requires the introduction of a larger number of auxiliary functions (see (3.16) and (3.23)), and becomes quite cumbersome. We do not proceed with the derivation of higher orders either, because retaining just the leading-order term in γ often provides quite an accurate solution (see appendix D).

https://doi.org/10.1017/jfm.2013.584 Published online by Cambridge University Press

Appendix C. Particular exactly solvable cases of the Sturm–Liouville boundary value problem (4.6)

C.1. *The 'top-hat' current*

For the case of a piecewise constant 'top-hat' current, $U = U_m$, $U_m < 0$ for $|y| < L$ and equal to zero for $|y| > L$, the eigenfunctions are constructed by matching sinusoidal and exponential functions at the points $y = \pm L$ (see e.g. Landau & Lifshitz 1977, § 22).

The modal function within the current is sinusoidal,

$$Y(y) \sim \cos(k_y y + \Theta_0), \quad |y| < L \quad \text{where } k_y = \sqrt{-l^2 - k^2 \frac{4kU_m}{\sqrt{kg}}} > 0, \tag{C 1}$$

and Θ_0 is a constant. Outside the domain of localization, $|y| > L$, the modal function decays exponentially:

$$Y(y) \sim \exp(\pm ly), \quad l > 0. \tag{C 2}$$

In the general case the solution is described by a transcendental equation. The eigenvalues l^2 are bounded by the condition

$$l^2 < -k^2 \frac{4kU_m}{\sqrt{kg}}. \tag{C 3}$$

For a sufficiently weak and narrow current in the sense that

$$\frac{|kU_m|}{\sqrt{kg}} \ll \frac{1}{k^2 L^2} \quad \text{which is equivalent to } \gamma \ll \mu^2, \tag{C 4}$$

the situation often referred to as a 'shallow potential', there is a single eigenvalue:

$$l^2 \approx k^2 \left(\frac{4kU_m}{\sqrt{kg}} kL \right)^2 \tag{C 5}$$

(see Landau & Lifshitz 1977, § 22, Problem 2).

In the opposite limit of a sufficiently strong and wide current, referred to as a 'deep potential well', the discrete eigenvalues are given by the explicit simple formula

$$l^2 = -4 \frac{k^3}{\sqrt{kg}} U_m - \frac{\pi^2 n^2}{L^2}, \quad n = 0, 1, \ldots, \ l > 0. \tag{C 6}$$

In this case the modal functions decay quickly outside the strip $|y| < L$, so that the waves are well-localized on the current.

C.2. *The* sech*-squared shape current*

When the lateral current shape is represented by the sech squared function, $U = U_0/\cosh^2(y/L)$, $U_0 < 0$, then (4.6) may be transformed into the general Legendre equation, which has solutions in the form of associated Legendre functions, P_r^s, as

$$Y = P_r^s \left(\tanh \frac{y}{L} \right) + (-1)^n P_r^s \left(-\tanh \frac{y}{L} \right), \tag{C 7}$$

$$r = -\frac{1}{2} + \frac{1}{2} \sqrt{1 - \frac{16k^3 U_0 L^2}{\sqrt{kg}}}, \quad s = lL. \tag{C 8}$$

The eigenmodes tend to zero as $y \to \pm\infty$, when condition $s = r - n$ is satisfied, where n is a non-negative integer (see e.g. Landau & Lifshitz 1977, § 23, Problem 5). Thus,

https://doi.org/10.1017/jfm.2013.584 Published online by Cambridge University Press

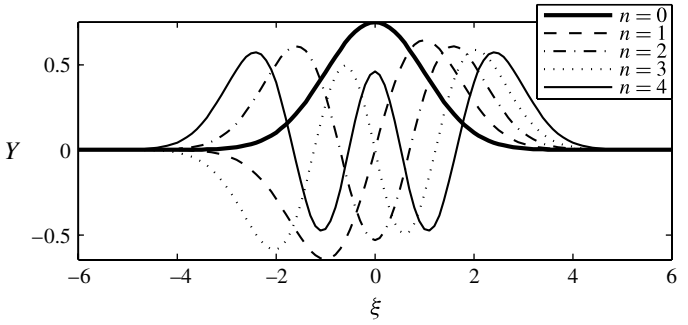


FIGURE 6. Normalized modes $Y_n(\xi)$ for the parabolic current. Five low modes are shown.

discrete eigenvalues corresponding to the trapped modes are given by the explicit formula

$$l^2 = \frac{1}{4L^2}\left[\sqrt{1 - \frac{16k^3U_0L^2}{\sqrt{kg}}} - (2n+1)\right]^2, \quad n = 0, 1, \ldots, l > 0. \tag{C 9}$$

The expression in square brackets should be positive; this condition bounds the number of existing tapped modes. The solution (C 7) may alternatively be represented in terms of hypergeometric functions (see Landau & Lifshitz 1977, § 23, Problem 5).

C.3. *The parabolic current*

An arbitrary smooth single-humped jet current may be approximated near the tip by a parabola, $U(y) = ay^2 + b$, where constants $a = U''/2$ and $b = U(0)$. For an opposite jet current $U(0) < 0$ and $U'' > 0$. Then the solution for (4.6) is given in terms of the Hermitian polynomials H_n (see Landau & Lifshitz 1977, § 23):

$$l^2 = -4\frac{k^3}{\sqrt{kg}}U(0) - (2n+1)\frac{k\sqrt{2kU''}}{\sqrt[4]{kg}}, \quad n = 0, 1, \ldots \tag{C 10}$$

$$Y = e^{-\xi^2/2}H_n(\xi), \quad \xi = y\frac{\sqrt{k}\sqrt[4]{2kU''}}{\sqrt[8]{kg}}. \tag{C 11}$$

The first five modes for the parabolic current are shown in figure 6. The eigenfunctions $Y(\xi)$ shown in the figure are normalized to ensure $\int_{-\infty}^{\infty} Y^2\,\mathrm{d}\xi = 1$.

The parabolic profile is not bounded in magnitude, and thus the assumption of a weak current becomes formally invalid for large $|y|$. However this profile is important, since in the vicinity of the tip any smooth single-humped jet current in the first approximation may be represented by a parabola. Then, solution (C 10) describes trapped modes which are well-localized near the tip of the current. This case corresponds to the 'shallow' energy levels of the parabolic potential well, that is, to the lowest modes and the maximal values of l^2.

For example, the sech-squared profile may be expanded in the Taylor series near $y = 0$ as $U \approx U_0(1 - (y/L)^2)$. It is easy to see that the exact eigenvalues for the sech-squared current (C 9) coincide with (C 10), when low modes are concerned, and when the total number of modes is large, so that condition (C 4) is inversed and we have a deep potential well.

https://doi.org/10.1017/jfm.2013.584 Published online by Cambridge University Press

C.4. *Asymmetric profiles: the triangular current*

All the examples examined so far have been symmetric, and it would be helpful to have an example of an asymmetric current. Consider the simplest 'triangular current' which models the situations of a current adjacent to a wall or a shore. The triangular current is defined as $U = ay$ for $-L < y < 0$ and is equal to zero outside the strip. Within the strip $-L < y < 0$, the boundary value problem (4.6) has a solution in the form of the Airy function,

$$Y \sim \mathrm{Ai}(D^{1/3}y + l^2 D^{-2/3}), \quad D \equiv \frac{4k^3 a}{\sqrt{kg}}. \tag{C 12}$$

On applying the boundary conditions on the eigenfunction on the left-hand side,

$$Y(-L) = 0, \tag{C 13}$$

we express the eigenvalues in terms of zeros of the Airy function, s_n,

$$l^2 = D^{1/3}L - s_n, \quad l > 0, \tag{C 14}$$

when a simplified condition at the point $y = 0$ is assumed (see Shrira & Townsend 2010). This assumption corresponds to the 'deep potential well' approximation. The values of s_n can be found explicitly by using the first term of the large n-asymptotic expansion (see Abramowitz & Stegun 1965)

$$s_n = \left[\frac{3\pi(4n+3)}{8}\right]^{2/3}, \quad n = 0, 1, \ldots. \tag{C 15}$$

Remarkably, this formula provides good accuracy starting with $n = 0$ (see Shrira & Townsend 2010). The analytic solution for the current with a trapezium cross-section may be obtained in a similar way.

An example of a smooth asymmetric profile of the current which admits an analytic solution is a generalization of the sech-squared profile: it is referred to as the Morse potential (Landau & Lifshitz 1977, § 23, Problem 4).

Appendix D. Accuracy of the Sturm–Liouville boundary value problem as a small γ limit for the broad current approximation

The boundary value problem for trapped modes (4.1) derived for $\mu \ll 1$ depends explicitly on parameter γ, which could in principle be arbitrary. In the limit of small γ, (4.1) reduces to the Sturm–Liouville boundary value problem (4.6). The crucial difference between the two is that the eigenfunctions of the Sturm–Liouville problem (4.6) are orthogonal and constitute a complete set, while the eigenfunctions of more general problem (4.1) are not orthogonal and it is not known whether or not they constitute a complete set. In view of further developments of the theory, our prime interest is in the modes' orthogonality, which is a key element for developing any theory based on the modal expansion. Here we are concerned with the question of major practical implications: when, i.e. for what range of γ, and with what accuracy we can use for problem (4.1) the dispersion relation and basis provided by (4.6). *A priori* it is not clear. In this section we examine the significance of non-orthogonality of the eigenfunctions for the non-classical problem (4.1) and show it to be negligible for a surprisingly large range of γ, at least for the examples we examined.

https://doi.org/10.1017/jfm.2013.584 Published online by Cambridge University Press

Consider first the Sturm–Liouville boundary value problem (4.6) with orthogonal eigenfunctions,

$$\overline{Y}'' + \overline{W}_n \overline{Y} = 0, \quad \overline{W}_n \equiv 4k^2 \left(\frac{\overline{\omega}_n - kU}{\sqrt{kg}} - 1 \right), \tag{D 1}$$

as the basis for studying problem (4.1), which we present here in the form

$$Y'' + W_n Y = 0, \quad W_n \equiv \frac{\Omega^4}{g^2} - k^2, \quad \Omega = \omega_n - kU. \tag{D 2}$$

The general boundary condition for (D 1) allowing for both trapped and passing-through modes is assumed, so that $\overline{Y}_n$ constitute a complete basis. We normalize the eigenfunctions in the standard fashion,

$$\int_{-\infty}^{\infty} \overline{Y}_n \overline{Y}_m \, \mathrm{d}y = \delta_{n,m}, \tag{D 3}$$

where $\delta_{n,m}$ is the Dirac delta function for the continuous spectrum and the Kronecker delta for the discrete modes.

Consider (D 2) to be a perturbation of problem (D 1). We specify the perturbation of the eigenmodes, ΔY_n, of the eigenvalues, $\Delta\omega_n$, and perturbation of $\overline{W}$, ΔW_n, as

$$\omega_n = \overline{\omega}_n + \Delta\omega_n, \quad Y_n = \overline{Y}_n + \Delta Y_n, \quad W_n = \overline{W}_n + \Delta W_n. \tag{D 4}$$

The perturbations are assumed to be in some sense small. We will discuss the necessary smallness later. A similar normalization is assumed for the perturbed eigenfunctions, $\int_{-\infty}^{\infty} Y_n^2 \, \mathrm{d}y = 1$. This normalization implies in the first approximation

$$\int_{-\infty}^{\infty} \Delta Y_n \overline{Y}_n \, \mathrm{d}y = 0 \tag{D 5}$$

(see also Landau & Lifshitz 1977, § 38).

Assuming $\Delta\omega_n$ to be small compared to $\overline{\Omega}_n$, the following expansion is justified:

$$\Omega_n^4 = (\overline{\Omega}_n + \Delta\omega_n)^4 = \overline{\Omega}_n^4 + 4\overline{\Omega}_n^3 \Delta\omega_n + O(\Delta\omega_n^2). \tag{D 6}$$

It is instructive to rewrite (D 1) in the form

$$\overline{\Omega}_n = \sqrt{kg} \left(1 - \frac{1}{4k^2} \frac{\overline{Y}_n''}{\overline{Y}_n} \right). \tag{D 7}$$

Making use of the small parameter χ, introduced by (3.17), which is the characteristic non-dimensional transverse wavenumber, $\overline{Y}_n'' \sim \chi^2 4k^2 \overline{Y}_n$, we can estimate $\overline{\Omega}_n^4$ as

$$\overline{\Omega}_n^4 = (kg)^2 \left(1 - \frac{1}{k^2} \frac{\overline{Y}_n''}{\overline{Y}_n} \right) + O(\chi^4). \tag{D 8}$$

Then, by virtue of (D 6) and (D 8), the boundary value problem (D 2) can be approximately presented as

$$\frac{Y_n''}{Y_n} - \frac{\overline{Y}_n''}{\overline{Y}_n} + 4\overline{\Omega}_n^3 \Delta\omega_n = O(\chi^4). \tag{D 9}$$

https://doi.org/10.1017/jfm.2013.584 Published online by Cambridge University Press

One particular solution to this relation is obvious:

$$Y_n = \overline{Y}_n + O(\chi^4) \quad \text{and} \quad \Delta\omega_n = O(\chi^4). \tag{D 10}$$

As shown in § 3, for each pair of k and ω_n problem (D 2) possesses only one trapped eigenmode, or a couple of passing modes; the latter may be specified uniquely by specifying the direction of propagation at the infinity.

Hence, $\overline{\Omega}_n$ and $\overline{Y}_n$ are very good approximations to Ω_n and Y_n as long as χ is small. We stress that smallness of χ does not necessarily imply smallness of γ. Indeed, according to estimates made in § 4.4, $\chi \sim \sqrt{\gamma}\,(n/N_{tr})^{1/2}$. Therefore χ is small either when $\gamma \ll 1$ and then $\chi^4 \sim \gamma^2$, or when $\mu \ll 1$ and n is not large, and then $\chi^4 \sim \gamma\mu^2$, and it may remain small even for $\gamma \sim 1$. Still, the accuracy has to be estimated quantitatively. To that end we apply a standard perturbation procedure in the spirit of Landau & Lifshitz (1977, § 38).

On multiplying (D 2) by $\overline{Y}_m$ and twice integrating the result by parts over the entire interval in y, we arrive at

$$\int_{-\infty}^{\infty} \left[Y_n \left(\overline{Y}_m'' + \overline{W}_n \overline{Y}_m \right) + \Delta W_n Y_n \overline{Y}_m \right] \mathrm{d}y = 0. \tag{D 11}$$

Using identity

$$\overline{W}_n = \overline{W}_m + \frac{4k^2}{\sqrt{kg}} (\overline{\omega}_n - \overline{\omega}_m) = \overline{W}_m + l_m^2 - l_n^2, \tag{D 12}$$

we immediately get

$$\left(l_m^2 - l_n^2\right) \int_{-\infty}^{\infty} Y_n \overline{Y}_m \,\mathrm{d}y + \int_{-\infty}^{\infty} \Delta W_n Y_n \overline{Y}_m \,\mathrm{d}y = 0. \tag{D 13}$$

These formulae enable us to expand the perturbations onto the orthonormal basis provided by (D 1) as follows:

$$\int_{-\infty}^{\infty} \Delta Y_n \overline{Y}_m \,\mathrm{d}y = \frac{1}{l_n^2 - l_m^2} \int_{-\infty}^{\infty} \Delta W_n Y_n \overline{Y}_m \,\mathrm{d}y, \quad n \neq m, \tag{D 14}$$

and

$$\int_{-\infty}^{\infty} \Delta W_n Y_n \overline{Y}_n \,\mathrm{d}y = 0, \quad n = m, \tag{D 15}$$

where

$$\Delta W_n = k^2 \left[\frac{(\overline{\omega}_n - kU)^4}{k^2 g^2} - 4\frac{\overline{\omega}_n - kU}{\sqrt{kg}} + 3 \right] + 4\frac{(\overline{\omega}_n - kU)^3}{g^2} \Delta\omega_n + O((\Delta\omega_n)^2). \tag{D 16}$$

Assuming the contribution due to ΔY_n to be small compared to that due to $\overline{Y}_n$, substitution of $\overline{Y}_n$ for Y_n into the integrals above yields the coefficients of expansion of the perturbations to the nth eigenfunction and the correction to the eigenvalue:

$$Y_n = \overline{Y}_n + \Delta Y_n, \quad \Delta Y_n = \Sigma_m d_{nm} \overline{Y}_m, \tag{D 17}$$

$$d_{nm} = \int_{-\infty}^{\infty} \Delta Y_n \overline{Y}_m \,\mathrm{d}y = \frac{1}{l_n^2 - l_m^2} \int_{-\infty}^{\infty} \Delta W_n \overline{Y}_n \overline{Y}_m \,\mathrm{d}y, \quad n \neq m, \tag{D 18}$$

https://doi.org/10.1017/jfm.2013.584 Published online by Cambridge University Press

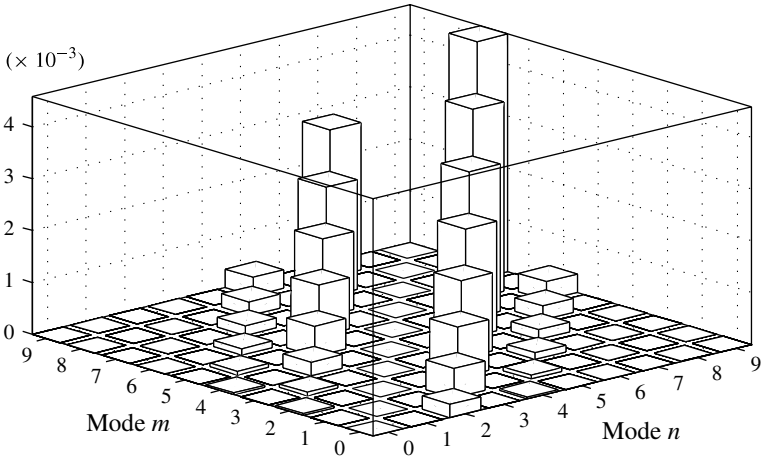


FIGURE 7. Integrals (D 18) computed for the ten lowest trapped modes for waves with period 6 s on the parabolic current $U = U_{max}\,(1 - y^2/L^2)$, where $U_{max} = -5$ m s^{-1} and $L = 25$ km.

$$\Delta\omega_n = \frac{\displaystyle\int_{-\infty}^{\infty} \left(4(\overline{\omega}_n - kU)(kg)^{3/2} - (\overline{\omega}_n - kU)^4 - 3k^2g^2\right)\overline{Y}^2\,\mathrm{d}y}{\displaystyle 4\int_{-\infty}^{\infty} (\overline{\omega}_n - kU)^3\overline{Y}^2\,\mathrm{d}y}, \tag{D 19}$$

where $d_{nn} = 0$ due to (D 5). Now we can justify our expansion *a posteriori*. As long as $\Delta\omega_n$ and expansion coefficients d_{nm} are small, we can use the results and properties of the Sturm–Liouville boundary value problem (4.6) with known accuracy.

Integrals (D 18) were computed numerically: $\omega_n = \overline{\omega}_n + \Delta\omega_n$ was used, and $\Delta\omega_n$ was estimated according to (D 19). For specific estimates we consider waves with longitudinal length of 60 m, which would correspond to ∼6 s freely propagating gravity waves.

For the first example we choose a parabolic current $U = U_{max}\,(1 - y^2/L^2)$ of unrealistically large magnitude $U_{max} = -5$ m s^{-1}, which for the chosen waves yields $\gamma \approx 0.5$. The width is taken to be similar to that of the tip of the Agulhas Current, $L = 25$ km. Then the frequencies of the trapped waves deviate considerably from the curve $\sqrt{kg}$, i.e. $\overline{\omega}/\sqrt{kg} \approx 0.5$; see the similar behaviour of the dispersion curves in figure 2(*d*). The values of d_{nm} are shown in figure 7, where modes n and m range from 0 to 9.

The two lowest approximate modes exhibit perfect agreement with the solution to (4.1). The discrepancy illustrated in figure 7 becomes visible, although still very small, starting from mode $n = 2$. Particular combinations of modes n and m result in somewhat larger values of integral (D 18), which is explained by specific symmetry features of the modes. The maximum of (D 18) for the ten lowest modes is found to be $\sim 5 \times 10^{-3}$. It increases when higher modes are considered: for fifty modes this quantity reaches the value of ∼0.13.

It was shown in § 4.5 (see figure 2*d*) that the solution of the Sturm–Liouville boundary value problem for weak currents (D 1) provides a very accurate approximation of the dispersion relation, even for quite strong currents. Estimate (D 19) for the considered parameters of the current results in the most significant correction of order $\Delta\omega_n/\overline{\omega}_n \sim -8 \times 10^{-6}$ (for the ninth mode $n = 9$).

https://doi.org/10.1017/jfm.2013.584 Published online by Cambridge University Press

Even if the current velocity is doubled, $U_{max} = 10$ m s^{-1}, and then $\gamma \sim 1$, the maxima for d_{nm} and $|\Delta\omega_n/\overline{\omega}_n|$ for the ten lowest modes are estimated in a similar way to 7×10^{-3} and 2.5×10^{-4}, respectively.

When, simultaneously, the current is significantly localized in the transverse dimension (μ is insufficiently small), the accuracy of the approximate problem (D 1) worsens considerably. For the third example, $U_{max} = 5$ m s^{-1} and $L = 300$ m ($\gamma \sim 0.5$, $\mu \sim 0.02$, corresponding to the case of shortest k in figure 2*d*) for the ten lowest modes $|d_{nm}| \lesssim 0.35$ and $|\Delta\omega_n/\overline{\omega}_n| \lesssim 0.03$.

Appendix E. Numerical solution of the original two-dimensional boundary value problem

Here we briefly describe the method we employed for solving the original two-dimensional boundary value problem specified by (3.2) and (3.7) with appropriate boundary conditions. First of all, we consider (3.2) in the water bulk to be a perturbation of the Helmholtz equation,

$$\frac{\partial^2\hat{w}}{\partial z^2} + \frac{\partial^2\hat{w}}{\partial y^2} - k^2\hat{w} = \left(2\frac{\Omega'^2}{\Omega^2} - \frac{\Omega''}{\Omega}\right)\hat{w}, \tag{E 1}$$

with boundary conditions

$$\Omega^2\hat{w} = g\frac{\partial\hat{w}}{\partial z} \quad \text{at } z = 0 \quad \text{and} \quad \hat{w} \to 0 \quad \text{as } z \to -\infty, \tag{E 2}$$

and

$$\hat{w}(y) \to 0 \quad \text{as } y \to \pm\infty. \tag{E 3}$$

We assume that the terms on the right-hand side of (E 1) are of order $\rho \equiv O(\gamma\mu^2) \ll 1$. Let

$$\hat{w} = \hat{w}^{(0)} + \rho\hat{w}^{(1)} + \rho^2\hat{w}^{(2)} + \cdots, \tag{E 4a}$$

$$\omega = \omega^{(0)} + \rho\omega^{(1)} + \rho^2\omega^{(2)} + \cdots. \tag{E 4b}$$

First consider

$$\frac{\partial^2\hat{w}^{(0)}}{\partial z^2} + \frac{\partial^2\hat{w}^{(0)}}{\partial y^2} - k^2\hat{w}^{(0)} = 0, \tag{E 5}$$

$$\Omega^{(0)2}\hat{w}^{(0)} = g\frac{\partial\hat{w}^{(0)}}{\partial z} \quad \text{at } z = 0 \quad \text{and} \quad \hat{w}^{(0)} \to 0 \quad \text{as } z \to -\infty. \tag{E 6}$$

Then we take the Fourier transform with respect to y:

$$F(l) = \mathscr{F}[f(y)] = \int_{-\infty}^{\infty} f(y)\mathrm{e}^{\mathrm{i}ly}\,\mathrm{d}y, \quad \mathscr{F}^{-1}[F(l)] = \frac{1}{2\pi}\int_{-\infty}^{\infty} F(l)\mathrm{e}^{-\mathrm{i}ly}\,\mathrm{d}l, \tag{E 7}$$

where $\mathscr{F}[\cdot]$ and $\mathscr{F}^{-1}[\cdot]$ are the operators of direct and inverse Fourier transform. Then, in terms of $W^{(0)}(l, z) \equiv \mathscr{F}[\hat{w}^{(0)}]$, (E 5) and (E 6) read

$$\frac{\partial^2 W^{(0)}}{\partial z^2} - m^2 W^{(0)} = 0 \quad \text{where } m \equiv \sqrt{k^2 + l^2}, \tag{E 8}$$

$$W^{(0)} * \mathscr{F}[\Omega^2(y)] = g\frac{\partial W^{(0)}}{\partial z} \quad \text{at } z = 0, \tag{E 9}$$

where $*$ means convolution.

https://doi.org/10.1017/jfm.2013.584 Published online by Cambridge University Press

The ansatz $W^{(0)}(l,z) = C^{(0)}(l)\mathrm{e}^{mz}$ corresponds to the fundamental solution of (E 8). The numerical procedure which solves (E 8) and (E 9) operates with N modes of the discrete Fourier transform. Condition (E 9) constrains unknown coefficients $C^{(0)}(l)$: for N unknowns there are N homogeneous algebraic equations. Non-degenerate solutions occur only when the determinant of the system of equations vanishes. Eigenfrequencies $\omega^{(0)}$ zeroing the determinant are sought within the interval $(\sqrt{kg} - |kU_{max}|, \sqrt{kg})$ by a two-stage search procedure with the computer round-off accuracy. When an eigenfrequency $\omega^{(0)}$ is found, a value is assigned to one of the coefficients $C^{(0)}(l)$, and then $N-1$ independent non-homogeneous algebraic equations on $N-1$ unknowns describe the desired mode:

$$\hat{w}^{(0)} = \mathscr{F}^{-1}\left[W^{(0)}(l,z)\right] = \frac{1}{2\pi}\int_{-\infty}^{\infty} C^{(0)}(l)\mathrm{e}^{mz}\mathrm{e}^{-\mathrm{i}ly}\,\mathrm{d}l. \tag{E 10}$$

Finally, the mode is normalized by requiring $\max|\hat{w}^{(0)}| = 1$. The numerically obtained solutions are found to be very accurate solutions of the problem (E 1)–(E 3).

Hence the zero-order problem specifies the eigenfunctions $\hat{w}^{(0)}$ and eigenvalues $\omega^{(0)}$. Assuming that the next-order in ρ corrections to $\hat{w}^{(0)}$ and $\omega^{(0)}$ are in some sense small, the next-order problem may be written down in the following form:

$$\frac{\partial^2\hat{w}^{(1)}}{\partial z^2} + \frac{\partial^2\hat{w}^{(1)}}{\partial y^2} - k^2\hat{w}^{(1)} = R\hat{w}^{(0)}, \tag{E 11}$$

where

$$R(y) \equiv \left(2\frac{\Omega^{(0)\prime}}{\Omega^{(0)2}} - \frac{\Omega^{(0)\prime\prime}}{\Omega^{(0)}}\right), \quad \Omega^{(0)} = \omega^{(0)} - kU. \tag{E 12}$$

The inhomogeneous ordinary differential (E 11) with fully determined right-hand side part may be solved straightforwardly by applying the Fourier transform with respect to y, $W^{(1)}(l,z) \equiv \mathscr{F}[\hat{w}^{(1)}]$,

$$\frac{\partial^2 W^{(1)}}{\partial z^2} - m^2 W^{(1)} = \mathscr{F}[R] * W^{(0)}, \tag{E 13}$$

$$W^{(1)} = \frac{\mathrm{e}^{mz}}{2m}\int f(\xi)\mathrm{e}^{-m\xi}\,\mathrm{d}\xi - \frac{\mathrm{e}^{-mz}}{2m}\int f(\xi)\mathrm{e}^{m\xi}\,\mathrm{d}\xi \equiv \hat{G}[f(z)],$$
$$\text{where} \quad f(z) \equiv \mathscr{F}[R] * W^{(0)}. \tag{E 14}$$

For the numerical solution, the discrete Fourier modes are given by

$$W^{(1)}(l) = \frac{R(l)C^{(0)}(l)}{2\sqrt{k^2+l^2}} z \exp\left(z\sqrt{k^2+l^2}\right)$$
$$+ \sum_{q\neq 0} \frac{R(l)C^{(0)}(l-q)}{(l-q)^2 - l^2} \exp\left(z\sqrt{k^2+(l-q)^2}\right) \quad \text{where } R(l) \equiv \mathscr{F}[R]. \tag{E 15}$$

We can introduce a shorthand operator $\hat{K}$ and rewrite the above as

$$\hat{w}^{(1)} = \hat{K}[\hat{w}^{(0)}]. \tag{E 16}$$

Then we can present $\hat{w}$ as the following series in ρ:

$$\hat{w} = \hat{w}^{(0)} + \hat{K}[\hat{w}^{(0)}] + \hat{K}[\hat{K}[\hat{w}^{(0)}]] + \cdots. \tag{E 17}$$

https://doi.org/10.1017/jfm.2013.584 Published online by Cambridge University Press

It is qualitatively different from the asymptotic series we have dealt with so far. It seems straightforward to show, as in Shrira (1993), that this series is absolutely convergent; however, the proof has not been carried out since it is lengthy and beyond the scope of the present paper. Assuming the convergence is proved, we can obtain a solution to (E 1) with any desired accuracy. Such a solution would be an exact solution of the equation, but not of the boundary value problem. We still have to satisfy the surface boundary condition and thus find the eigenvalues. To that end we have to satisfy

$$g\frac{\partial \hat{w}^{(1)}}{\partial z} = \Omega^{(0)2}\hat{w}^{(1)} + 2\Omega^{(0)}\omega^{(1)}\hat{w}^{(0)} \quad \text{at } z = 0. \tag{E 18}$$

Since $\Omega(y)$ does not tend to zero anywhere, one may obtain from (E 18)

$$\omega^{(1)} = \frac{\displaystyle\int_{-\infty}^{\infty}\left(g\frac{\partial \hat{w}^{(0)}}{\partial z} - \Omega^{(0)2}\hat{w}^{(0)}\right)\frac{\hat{w}^{(0)}}{2\Omega^{(0)}}\,\mathrm{d}y}{\displaystyle\int_{-\infty}^{\infty}\hat{w}^{(0)2}\,\mathrm{d}y} \quad \text{at } z = 0. \tag{E 19}$$

Note that corrections to the eigenfrequency modify the kernel $\hat{K}$ at each step of the iterations (E 17), hence the development of a higher-order perturbation theory is in fact more complicated.

The first-order solution, $\hat{w} = \hat{w}^{(0)} + \hat{w}^{(1)}$ and $\omega = \omega^{(0)} + \omega^{(1)}$, found numerically, proved to be sufficiently accurate to be used in § 5 (see the upper surface in figure 3*b*) for validation of the asymptotic approach. In the case of a sech-squared current with $U_0 = -5$ m s^{-1}, $L = 200$ m for $k = 0.1$ rad m^{-1}, the maximum amplitude of the correction $\hat{w}^{(1)}$ for the lowest 30 modes is within the range $2 \ldots 7\,\%$ of amplitude $\hat{w}^{(0)}$. When the correction significance is estimated using

$$\frac{\displaystyle\int_{-\infty}^{0}\int_{-\infty}^{\infty}\left[\left(\hat{w}^{(0)} + \hat{w}^{(1)}\right)^2 - \hat{w}^{(0)2}\right]\mathrm{d}y\,\mathrm{d}z}{\displaystyle\int_{-\infty}^{0}\int_{-\infty}^{\infty}\hat{w}^{(0)2}\,\mathrm{d}y\,\mathrm{d}z}, \tag{E 20}$$

this results in values in the range $1 \times 10^{-3} \ldots 7 \times 10^{-2}$. This correction improves the accuracy in satisfying (E 1) by the numerical solution by up to two orders. The correction to eigenfrequency $\omega^{(1)}$ (E 19) improves the accuracy in satisfying the boundary condition (E 2) compared to eigenfrequency $\omega^{(0)}$. This correction is found to be less than $1.2 \times 10^{-3}|kU_{max}|$.

REFERENCES

Abramowitz, M. & Stegun, I. A. 1965 *Handbook of Mathematical Functions*. Dover.

Bühler, O. 2009 *Waves and Mean Flows*. Cambridge University Press.

Dalrymple, R. A., MacMahan, J. H., Reniers, A. J. H. M. & Nelko, V. 2011 Rip currents. *Annu. Rev. Fluid Mech.* **43**, 551–581.

Drazin, P. G. & Johnson, R. S. 1989 *Solitons: An Introduction*. Cambridge University Press.

Galvin, C. J. 1967 Longshore current velocity: a review of theory and data. *Rev. Geophys.* **5** (3), 287–304.

Gerber, M. 1987 The Benjamin–Feir instability of a deep-water Stokes wavepacket in the presence of a non-uniform medium. *J. Fluid Mech.* **176**, 311–332.

https://doi.org/10.1017/jfm.2013.584 Published online by Cambridge University Press

HJELMERVIK, K. B. & TRULSEN, K. 2009 Freak wave statistics on collinear currents. *J. Fluid Mech.* **637**, 267–284.

IRVINE, D. E. & TILLEY, D. G. 1988 Ocean wave directional spectra and wave–current interaction in the Agulhas from the Shuttle Imaging Radar-B synthetic aperture radar. *J. Geophys. Res.* **93** (C12), 15389–15401.

JONSSON, I. G. 1990 Wave–current interactions. In *The Sea, 9A: Ocean Engineering Science* (ed. B. le Méhauté & D. M. Hanes), pp. 65–120. Wiley Interscience.

KENYON, K. E. 1971 Wave refraction in ocean currents. *Deep-Sea Res.* **18**, 1023–1034.

KOMEN, G. J., CAVALERI, L., DONELAN, M., HASSELMANN, K., HASSELMANN, S. & JANSSEN, P. A. E. M. 1996 *Dynamics and Modelling of Ocean Waves*. Cambridge University Press.

KUDRYAVTSEV, V. N., GRODSKY, S. A., DULOV, V. A. & BOL'SHAKOV, A. N. 1995 Observations of wind waves in the Gulf Stream frontal zone. *J. Geophys. Res.* **100** (C10), 20715–20727.

LANDAU, L. D. & LIFSHITZ, E. M. 1977 *Quantum Mechanics*. Non-Relativistic Theory, vol. 3, Pergamon.

LAVRENOV, I. 1998 The wave energy concentration at the Agulhas Current of South Africa. *Nat. Hazards* **17**, 117–127.

LAVRENOV, I. V. 2003 *Wind Waves in Ocean: Dynamics and Numerical Simulations*. Springer.

LIGHTHILL, J. 2001 *Waves in Fluids*. Cambridge Mathematical Library Series, Cambridge University Press.

LUTJEHARMS, J. R. E. 2006 *The Agulhas Current*. Springer.

MALLORY, J. K. 1974 Abnormal waves on the South East coast of South Africa. *Intl Hydrographic Rev.* **51**, 99–129.

MCKEE, W. D. 1974 Waves on a shearing current: a uniformly valid asymptotic solution. *Proc. Camb. Phil. Soc.* **75**, 295–301.

MEI, C. C., STIASSNIE, M. & YUE, D. K.-P. 2005 *Theory and Applications of Ocean Surface Waves. Part 1: Linear Aspects*. World Scientific.

ONORATO, M., PROMENT, D. & TOFFOLI, A. 2011 Triggering rogue waves in opposing currents. *Phys. Rev. Lett.* **107**, 184502.

ORSI, A. H., WHITWORTH, T. & NOWLIN, W. D. 1995 On the meridional extent and fronts of the Antarctic Circumpolar Current. *Deep-Sea Res.* **42** (5), 641–673.

PEREGRINE, D. H. 1976 Interaction of water waves and currents. *Adv. Appl. Maths* **16**, 9–117.

PEREGRINE, D. H. & SMITH, R. 1975 Stationary gravity waves on non-uniform free streams: jet-like streams. *Math. Proc. Camb. Phil. Soc.* **77**, 415–438.

PHILLIPS, O. M. 1966 *The Dynamics of the Upper Ocean*. Cambridge University Press.

RINTOUL, S. R., HUGHES, C. W. & OLBERS, D. 2001 The antarctic circumpolar current system. In *International Geophysics*, chap. 4.6, Ocean Circulation and Climate: Observing and Modelling the Global Ocean, vol. 77, pp. 271–302. Elsevier, XXIX–XXXVI.

RUBAN, V. P. 2012 On the nonlinear Schrödinger equation for waves on a non-uniform current. *J. Expl Theor. Phys. Lett.* **95**, 486–491.

SHRIRA, V. I. 1993 Surface waves on shear current: solution of the boundary-value problem. *J. Fluid Mech.* **252**, 565–584.

SHRIRA, V. I. & TOWNSEND, W. A. 2010 Inertia-gravity waves beyond the inertial latitude. Part 1. Inviscid singular focusing. *J. Fluid Mech.* **664**, 478–509.

SIMON, B. 1976 The bound state of weakly coupled Schrödinger operators in one and two dimensions. *Ann. Phys.* **97**, 279–288.

SMITH, R. 1970 Asymptotic solutions for high-frequency trapped wave propagation. *Phil. Trans. R. Soc. Lond. Ser.* A **268**, 289–324.

SMITH, R. 1975 The reflection of short gravity waves on a non-uniform current. *Math. Proc. Camb. Phil. Soc.* **78**, 517–525.

SMITH, R. 1976 Giant waves. *J. Fluid Mech.* **77**, 417–431.

STOCKER, J. D. & PEREGRINE, D. H. 1999 The current-modified nonlinear Schrödinger equation. *J. Fluid Mech.* **399**, 335–353.

https://doi.org/10.1017/jfm.2013.584 Published online by Cambridge University Press

THORNTON, E. B. & GUZA, R. T. 1986 Surf zone longshore currents and random waves: field data and models. *J. Phys. Oceanogr.* **16**, 1165–1178.

THOMAS, G. P. 1981 Wave-current interactions: an experimental and numerical study. Part 1. Linear waves. *J. Fluid Mech.* **110**, 457–474.

THOMAS, G. P. & KLOPMAN, G. 1997 Wave-current interactions in the near-shore region. In *Advances in Fluid Mechanics*, pp. 255–319. Computational Mechanics Publications.

TOOLE, J. M. & RAYMER, M. E. 1985 Heat and fresh water budgets of the Indian Ocean. *Deep-Sea Res.* A **32**, 917–928.

TURPIN, F.-M., BENMOUSSA, C. & MEI, C. C. 1983 Effects of slowly varying depth and current on the evolution of a Stokes wavepacket. *J. Fluid Mech.* **132**, 1–23.

https://doi.org/10.1017/jfm.2013.584 Published online by Cambridge University Press